



# Identification of NO<sub>2</sub> and SO<sub>2</sub> over China: Characterization of polluted and hotspots Provinces

Md. Arfan Ali<sup>1,2</sup> · Mazen E. Assiri<sup>2,3</sup> · M. Nazrul Islam<sup>4</sup> · Muhamad Bilal<sup>5</sup> · Ayman Ghulam<sup>6</sup> · Zhongwei Huang<sup>1</sup>

Received: 21 January 2024 / Accepted: 3 April 2024 / Published online: 30 April 2024  
© The Author(s), under exclusive licence to Springer Nature B.V. 2024

## Abstract

Increasing emissions of aerosol and trace gases (e.g. nitrogen dioxide: NO<sub>2</sub> and sulfur dioxide: SO<sub>2</sub>) have resulted in severe air pollution in China due to its rapid industrialization, economic growth, and urbanization. This resulted in numerous environmental and health problems, and poor air quality mainly in industrial areas and major cities. This study identifies long-term (2005–2020) Ozone Monitoring Instrument (OMI) based NO<sub>2</sub> and SO<sub>2</sub> pollution hotspots across China by analyzing spatiotemporal distributions and variations, with characterization of polluted provinces, SO<sub>2</sub>/NO<sub>2</sub> ratio, trend, and assessing how effective China's Air Pollution Control Policy (APCP) is on NO<sub>2</sub> and SO<sub>2</sub>. Results show that NO<sub>2</sub> and SO<sub>2</sub> pollution hotspots were seen in China's central (Hubei), eastern (Anhui, Jiangsu, Shandong, Zhejiang), northern (Beijing, Hebei, Henan, Shanxi, Tianjin), northeast (Liaoning, Jilin), northwestern (Urumqi), southern (Guangdong, Hong Kong), and southwest (Chongqing, Sichuan). However, the pollution level was higher in winter, followed by autumn, spring, and summer. China's eight provinces (Tianjin, Shanghai, Shandong, Jiangsu, Beijing, Hebei, Hong Kong, and Henan) were identified as extremely polluted with high NO<sub>2</sub> levels ranging from 16.86–9.75 (10<sup>15</sup> molecules/cm<sup>2</sup>), whereas Shandong, Tianjin, Hebei, Beijing, Henan, Shanxi, Jiangsu, Shanghai, Anhui, and Liaoning were deemed to extremely polluted provinces with high SO<sub>2</sub> levels ranging from 20.62–14.30 (10<sup>15</sup> molecules/cm<sup>2</sup>). Moreover, the SO<sub>2</sub>/NO<sub>2</sub> ratio for 27 Chinese provinces fluctuates between 1.02 to 4.98, indicating industries emit more SO<sub>2</sub> than NO<sub>2</sub>. Finally, China's air pollution control policies (APCP) led to the largest annual reductions in NO<sub>2</sub> during the 12th five-year plan (FYP) (6%–94%) and SO<sub>2</sub> during the 11th FYP (6%–74%). The present study concludes, however, that China's APCP improved air quality by easing NO<sub>2</sub> and SO<sub>2</sub> emissions. This study recommends that the Chinese government may adopt a comprehensive strategy to reduce air pollution, including investing in clean energy, promoting electric vehicles, enforcing strict emission standards for industries, implementing green building practices, and raising public awareness about pollution reduction.

**Keywords** Aura · OMI · NO<sub>2</sub> Pollutant · SO<sub>2</sub> Pollutant · Hotspots · Trend

## Introduction

Air pollution in China has been compounded by rapid industrialization, socioeconomic development, urbanization, agricultural revolution, and meteorological factors

(Chan and Yao 2008; de Leeuw et al. 2021; Wei et al. 2023). There are many harmful impacts of air pollution, including harming human health, affecting food security, hindering economic development, influencing climate change, and negatively impacting the environment (Wang

✉ Md. Arfan Ali  
arfan.ray@gmail.com

✉ Zhongwei Huang  
huangzhongwei@lzu.edu.cn

<sup>1</sup> The Regional Center for Climate Change, National Center for Meteorology, Jeddah 21431, Saudi Arabia

<sup>2</sup> Collaborative Innovation Center for West Ecological Safety (CIWES), Key Laboratory for Semi-Arid Climate Change of the Ministry of Education, College of Atmospheric Sciences, Lanzhou University, Lanzhou 730000, China

<sup>3</sup> Department of Meteorology, King Abdulaziz University, Jeddah 21589, Saudi Arabia

<sup>4</sup> Climate Services Department, National Center for Meteorology, Jeddah 21431, Saudi Arabia

<sup>5</sup> Center for Sustainability and the Global Environment (SAGE), Nelson Institute for Environmental Studies, University of Wisconsin—Madison, Madison, USA

<sup>6</sup> National Center for Meteorology, Jeddah 21431, Saudi Arabia

et al. 2012; UNECE 2021; Hao et al. 2014). Air pollution occurs from various natural and anthropogenic sources: natural sources like volcanoes, fires, sand and dust storms, gas extraction, and marshlands (Zhang et al. 2008; Wang et al. 2011; Lin and McElroy 2011; Hilboll et al. 2013; Lu et al. 2013; Guo et al. 2019; Zheng et al. 2018), while anthropogenic sources like transport, agriculture, industry, municipal infrastructure, and possesses related to fuel extraction and combustion (Levelt et al. 2006a, b and 2018; Munro et al. 2016; Damiani et al. 2012; Celarier et al. 2008; Veeffkind et al. 2012). However, the primary contributors to air pollution are aerosol and gaseous pollutants such as aerosol optical depth (AOD), particulate matter (PM), ozone (O<sub>3</sub>), nitrogen dioxide (NO<sub>2</sub>), and sulfur dioxide (SO<sub>2</sub>) (Wang et al. 2021a). Worth noting that the two atmospheric trace gases NO<sub>2</sub> and SO<sub>2</sub> play a significant role in chemical reactions associated with air pollution and reduce the air quality, along with producing acid rain, haze and photochemical smog therefore consideration them for policy implications of a nation (Shon et al. 2011).

Among the variety of substances contributing to atmospheric pollution, a subset originates predominantly from anthropogenic sources, classified as characteristic pollutants. These encompass gaseous pollutants, such as chemical compounds including gases and vapors (e.g. carbon oxides: CO and CO<sub>2</sub>, sulfur oxides: SO<sub>2</sub> and SO<sub>3</sub>, and nitrogen oxides: NO and NO<sub>2</sub>); solid particles (PM<sub>2.5</sub> and PM<sub>10</sub>); liquid droplets; and biochemical contaminants (microorganisms like viruses, bacteria, and fungi). Despite preventive measures being discussed by different countries and international bodies, there is a greater possibility of anthropogenic pollutants increasing with climate change (Abbass et al. 2022). Not only natural and anthropogenic pollutants, but military activity also has significant impacts on the environment (Saxena 2023). Recent and ongoing military activities in the war areas of the world produce extensive amounts of greenhouse gases, pollution, and cause resource depletion among other environmental impacts (Shukla et al. 2023). Further, contaminating the environment is caused by using explosive weapons, which release toxic and hazardous chemicals from damaged infrastructure (Shukla et al. 2023). Primary pollutants as well as their chemical reactions with atmospheric components result in the formation of secondary pollutants often more hazardous than their primary counterparts (Yuan et al. 2012). As pollutants in the atmosphere do not follow political borders, they can travel from one region to another in the world, which means there is a connection between warfare and air pollution (UNECE 2021; Chang 2012; Slezakova et al. 2011). Since pollutants affect air quality, climate, human health, terrestrial acidification, and marine ecosystems (Berglen 2004; Seinfeld and Pandis

2006), this study focuses on the two most important pollutants in 33 provinces of China: NO<sub>2</sub> and SO<sub>2</sub>.

Monitoring and protecting air quality is challenging due to the dynamic nature of NO<sub>2</sub> and SO<sub>2</sub>, and their dispersion and environmental exchange (Wang et al. 2021a). Based on the diverse modes of pollutant dispersion, sources are categorized into points, linear, and surface. There are several technical parameters determining pollutant spread; however, emission volume and the nature of emitted pollutants are crucial. Alongside emitter technicalities, meteorological conditions, encompassing air temperature, wind speed and direction, and precipitation, significantly influence pollutant spread, which may vary from province to province in China. It has been well established that NO<sub>2</sub> and SO<sub>2</sub> have significant impacts on human health and plants, and many researchers have used satellite and ground-based observations to investigate the characteristics of these pollutants (Zhang et al. 2017; Krotkov et al. 2016; Haq et al. 2015; Zheng et al. 2018; Wang et al. 2021a; Ali et al. 2023b).

However, ground-based measurements give insights into the temporal distribution and impact of NO<sub>2</sub> and SO<sub>2</sub> pollutants on human health and climate (Zhang et al. 2017; Zheng et al. 2018; Ali et al. 2023b). In the current world, there are limited numbers of ground-based air pollution recording stations, which provide inadequate observations over a short period. In this circumstance, satellite observations overcome this pollution data recording limitation and provide long-term observations of NO<sub>2</sub> and SO<sub>2</sub>. Several satellite-based sensors such as the Global Ozone Monitoring Experiment (GOME) instrument (Burrows et al. 1999; Eisinger and Burrows 1998), the Scanning Imaging Absorption Spectrometer for Atmospheric Chartography (SCIAMACHY) (Bovensmann et al. 1999), GOME-2 (Callies et al. 2004; Munro et al. 2016), Ozone Monitoring Instrument (OMI) (Levelt et al. 2006a, b), and Tropospheric Monitoring Instrument (TROPOMI) (Veeffkind et al. 2012) have been designed and launched for measuring atmospheric gaseous pollutants. As documented by Krotkov et al. (2016) and Levelt et al. (2018), OMI stands out as a frequently utilized used sensor, with its 13 km × 24 km nadir spatial resolution and 98.8-min temporal resolution. However, this sensor is widely used for air quality monitoring, ozone detection, and volcanic gas detection and quantification (Levelt et al. 2018). The OMI-based NO<sub>2</sub> and SO<sub>2</sub> over Asia, United States of America, and Europe were investigated by Krotkov et al. (2016) who found that both increasing and decreasing trends. Throughout 12-year, Haq et al. (2015) studied the spatio-temporal distributions and variations of NO<sub>2</sub> and SO<sub>2</sub>, and their trends over South Asia. However, air pollution has been studied in China in several ways, including prolonged exposure to NO<sub>2</sub> and SO<sub>2</sub> leads to increased mortality rates (Carey et al. 2013; Tao et al. 2012), long-term exposure to NO<sub>2</sub> rises higher respiratory and cardiovascular mortality rates (Dong et al. 2012), NO<sub>2</sub>

and SO<sub>2</sub> observed using ship-based and satellite observations over East China (Tan et al. 2018), spatiotemporal variations of ground-based CO, NO<sub>2</sub>, and SO<sub>2</sub> over China (Wei et al. 2023), and Beijing (He et al. 2023), and NO<sub>2</sub> and SO<sub>2</sub> hot-spots, variations, trends and their potential sources identified over only Jiangsu province (Ali et al. 2023b). Therefore, the present study focused on spatio-temporal distributions, variability, characterization of polluted provinces, SO<sub>2</sub>/NO<sub>2</sub> ratio, and trends of NO<sub>2</sub> and SO<sub>2</sub> pollution over 33 provinces in China using satellite observations from 2005–2020. This research provides policy recommendations on air pollution for 33 provinces in China.

## Data and methods

### Study area

This study only focuses on China mainland (Latitude: 3°51′–53°33′ N and Longitude: 73°33′–135°05′ E), which is the world's most populous country (e.g. 1.4 billion). The country has a varied climate and distinct geography with complex topography, desert and forest landscapes, coastal and surrounding areas, densely populated and under-populated regions. China is divided into 22 provinces (e.g. Anhui, Fujian, Gansu, Guangdong, Guizhou, Hainan, Heilongjiang, Henan, Hubei, Hunan, Jiangsu, Jiangxi, Jilin, Liaoning, Qinghai, Shaanxi, Shandong, Shanxi, Sichuan, Yunnan, and Zhejiang), with four municipalities (e.g. Beijing, Chongqing, Shanghai, and Tianjin) and five autonomous regions (e.g. Guangxi, Inner-Mongolia, Ningxia, Xinjiang, and Tibet) (Fig. 1). This

study considers four municipalities, two special administrative regions, and five autonomous regions to be provinces (a total of 33 provinces). Major sources of anthropogenic emissions in China include industrial activities and urbanization, along with extensive transportation actions. Aerosol concentrations are further heightened by natural emissions such as dust from deserts in the north and west of the country and precursor gases from biological emissions, forest fires, and agriculture emissions. The North China Plain (NCP: parts of Henan, Hebei, Shandong, Jiangsu, and Anhui provinces), Yangtze River Delta (YRD: parts of Anhui, Jiangsu, Zhejiang, and Shanghai), Central, and Pearl River Delta (PRD: Guangdong, Hong Kong, and Macau provinces) regions stand out as the most populated, urbanized, and industrialized areas in China, leading to elevated levels of anthropogenic emissions. A mountainous terrain, a low population density, and anthropogenic activity distinguish Tibet and Qinghai in China.

### OMI NO<sub>2</sub> and SO<sub>2</sub> products

The OMI is a sensor onboard the Aura satellite and passes the equator at a local time 13:45 pm while maintaining an altitude of 705 km above the earth's surface. The National Aeronautics and Space Administration (NASA) deployed the sensor on 15 July 2004, in collaboration with Finland, the United Kingdom, and the Netherlands. This sensor measures reflected solar radiation based on wavelengths ranging from 250–500 nm with a spatial resolution of 13 × 15 km at nadir (Levelt et al. 2006a). In the OMI, the near-ultraviolet aerosol retrieval (OMAERUV) algorithm is used to retrieve absorbing aerosols (e.g. dust and smoke or carbonaceous aerosols)

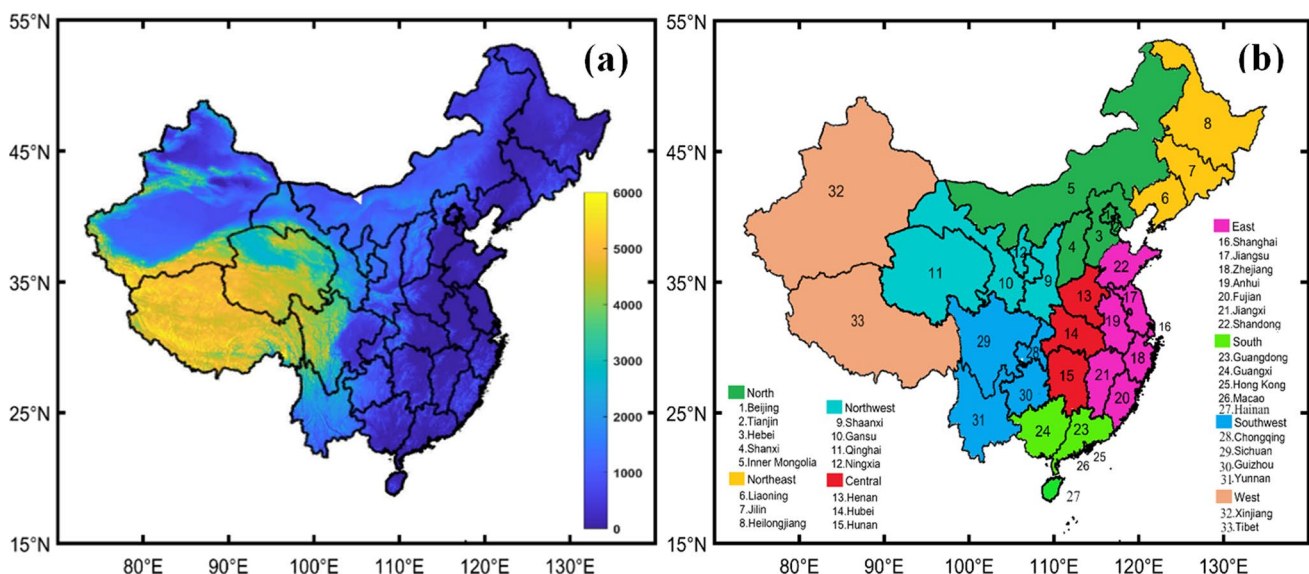


**Fig. 1** Geographical map of China mainland **a**) elevation map (m) and **b**) provinces, municipalities, special administrative, and autonomous regions

(Torres et al. 2007) such as absorption aerosol optical depth (AAOD) and aerosol index (UVAI) products. The algorithms use UV spectral region of the OMI to measure total and tropospheric column densities of trace gases (NO<sub>2</sub> and SO<sub>2</sub>) (Carn et al. 2017; Krotkov et al. 2016). In this study, daily tropospheric vertical column density (TVCD) for NO<sub>2</sub> (OMNO2e: cloud fraction < 30%) and VCD SO<sub>2</sub> (OMSO2e: cloud fraction radiance: < 0.2) data were obtained from OMI version-3 and level-3 with a spatial resolution of 0.25° × 0.25°.

## Methodology

The present study applied the following step-by-step methods to achieve each objective:

- The 16-year (2005 – 2020) spatial distribution and area-averaged maps of NO<sub>2</sub> and SO<sub>2</sub> on annual, seasonal, and monthly scales were generated from monthly OMI products. Moreover, 33 province's shape files were used to extract area averaged NO<sub>2</sub> and SO<sub>2</sub>.
- A quartile technique was used to characterize and ranking of extremely polluted provinces in China. Using the first (Q1) and third (Q3) quartiles, polluted and extremely polluted provinces were defined. NO<sub>2</sub> and SO<sub>2</sub> levels between the first and third quartiles were generally considered as highly polluted provinces. A previous study also used this technique to define polluted, highly polluted, and extremely polluted cities in Pakistan (Bilal et al. 2021). For example, NO<sub>2</sub> < 2 (Q1) and SO<sub>2</sub> < 9 (Q1) represent less polluted provinces, 2 ≤ NO<sub>2</sub> ≤ 9 and 9 ≤ SO<sub>2</sub> ≤ 14 represent highly polluted provinces, and NO<sub>2</sub> > 9 (Q3) and SO<sub>2</sub> > 14 (Q3) represent extremely polluted provinces.
- The SO<sub>2</sub>/NO<sub>2</sub> ratio identifies NO<sub>2</sub> and SO<sub>2</sub> emission sources in China, regardless of whether they are from

mobile (traffic emissions) or point sources (industrial activities). However, the SO<sub>2</sub>/NO<sub>2</sub> ratio > 0.6 indicates significant emissions from industrial activities, whereas that of greater than 1.5 signifies high-sulfur fuel content emissions from ships (Ali et al. 2023b; Wang et al. 2021a).

- For trend calculation, seasonality was effectively deleted from time series using mean annual cycle (MAC) and annual cycle using singular spectrum analysis (SSA). The seasonal adjusted time series (A) was calculated based on the following Eq. (1):

$$A = Y - S \quad (1)$$

Here, Y belongs to the original time series of NO<sub>2</sub> and SO<sub>2</sub>, and S defines the seasonal cycle. The Ordinary Least Square (OLR) regression was applied to compute the slope (α<sub>2</sub>) and breakpoint from the seasonal adjusted time series (Eq. 2):

$$A = \alpha_1 + \alpha_2 t + \varepsilon_t \quad (2)$$

Here, α<sub>1</sub> and ε<sub>t</sub> define respectively the intercept and residual error (Verbesselt et al. 2012). However, Forkel et al. (2013) provides more information on slope and breakpoint computation.

- To assess the robustness of OLS-based trends, the study uses the Theil-Sen's Slope (Sen 1968; Theil 1992) combined with the Mann-Kendall (MK) test (Kendall 1975; Mann 1945). A two-tailed test was used to determine the significance (at 95% confidence level) of NO<sub>2</sub> and SO<sub>2</sub> trends. In order to compare the NO<sub>2</sub> and SO<sub>2</sub> trends in 33 provinces, this study computed the percent change in NO<sub>2</sub> and SO<sub>2</sub> (Eq. 3) because of the high seasonal discrepancy in China.

$$\text{PercentChange}(\%) = \frac{\text{Trend} \times \text{total numbers of year}}{\text{Long-term Mean of NO}_2 \text{ and SO}_2} \times 100 \quad (3)$$

However, several earlier studies were used this technique to present the changes in aerosols and gaseous pollutants (Ali et al. 2023a; Mhawish et al. 2021; Sogacheva et al. 2018; Yue and Hashino 2003; Wang et al. 2021b).

## Results

### Spatial distributions of NO<sub>2</sub> and SO<sub>2</sub>

The main sources of NO<sub>2</sub> are fossil fuel combustion, industrial emissions, automobile emissions, biomass burning, natural lightning, and soil microbe emissions (Bilal et al. 2021;

Cheng et al. 2012; Lee et al. 1997; Richter and Burrows 2002). In contrast, the main sources of SO<sub>2</sub> are volcanoes, coal, oil and gas, and smelters (Dahiya and Myllyvirta 2019). The spatial distributions of the annually, seasonally, and monthly averaged NO<sub>2</sub> and SO<sub>2</sub> from Aura-based OMI over China are consistent, with higher NO<sub>2</sub> and SO<sub>2</sub> across the central, eastern, northeast, northwestern, south, and southwest regions (Figs. 2, 3 and S1). However, most regions of China including across the central (Hubei), eastern (Jiangsu, Anhui, Zhejiang), north (Beijing, Hebei, Henan, Inner Mongolia, Shandong, Shanxi, Shaanxi, Tianjin), northeast (Liaoning, Jilin), northwestern (Urumqi), South (Guangdong, Hong Kong), and southwest (Chongqing, Sichuan)

experienced annually higher levels of  $\text{NO}_2$  ( $> 5 \times 10^{15}$  molecules/cm<sup>2</sup>) and  $\text{SO}_2$  ( $> 8 \times 10^{15}$  molecules/cm<sup>2</sup>), signifying as the largest polluted areas in the country. Additionally, annually second-highest levels of  $\text{NO}_2$  ( $1.01\text{--}5.00 \times 10^{15}$  molecules/cm<sup>2</sup>) were evident over the parts of Fujian, Gansu, Guangxi, Guizhou, Hainan, Heilongjiang, Hunan, Inner Mongolia, Jiangxi, Jilin, Ningxia, and Xinjiang (Fig. 2), whereas  $\text{SO}_2$  ( $2.01\text{--}8.00 \times 10^{15}$  molecules/cm<sup>2</sup>) were observed over the parts of Gansu, Hainan, Inner Mongolia,

Qinghai, Tibetan Plateau, Xinjiang, and Yunnan (Fig. 3). Notably, lower levels of  $\text{NO}_2$  ( $< 1 \times 10^{15}$  molecules/cm<sup>2</sup>) were observed across the Qinghai and Tibetan Plateau with over the parts of Gansu, Inner Mongolia, Sichuan, and Yunnan, mainly due to the lower primary emissions and good atmospheric ventilation. Furthermore, significant year-to-year spatial variations in  $\text{NO}_2$  and  $\text{SO}_2$  were observed over China from 2005–2020 (Figs. S1–S2). Across the highly-polluted regions of China, uncontrolled economic growth,

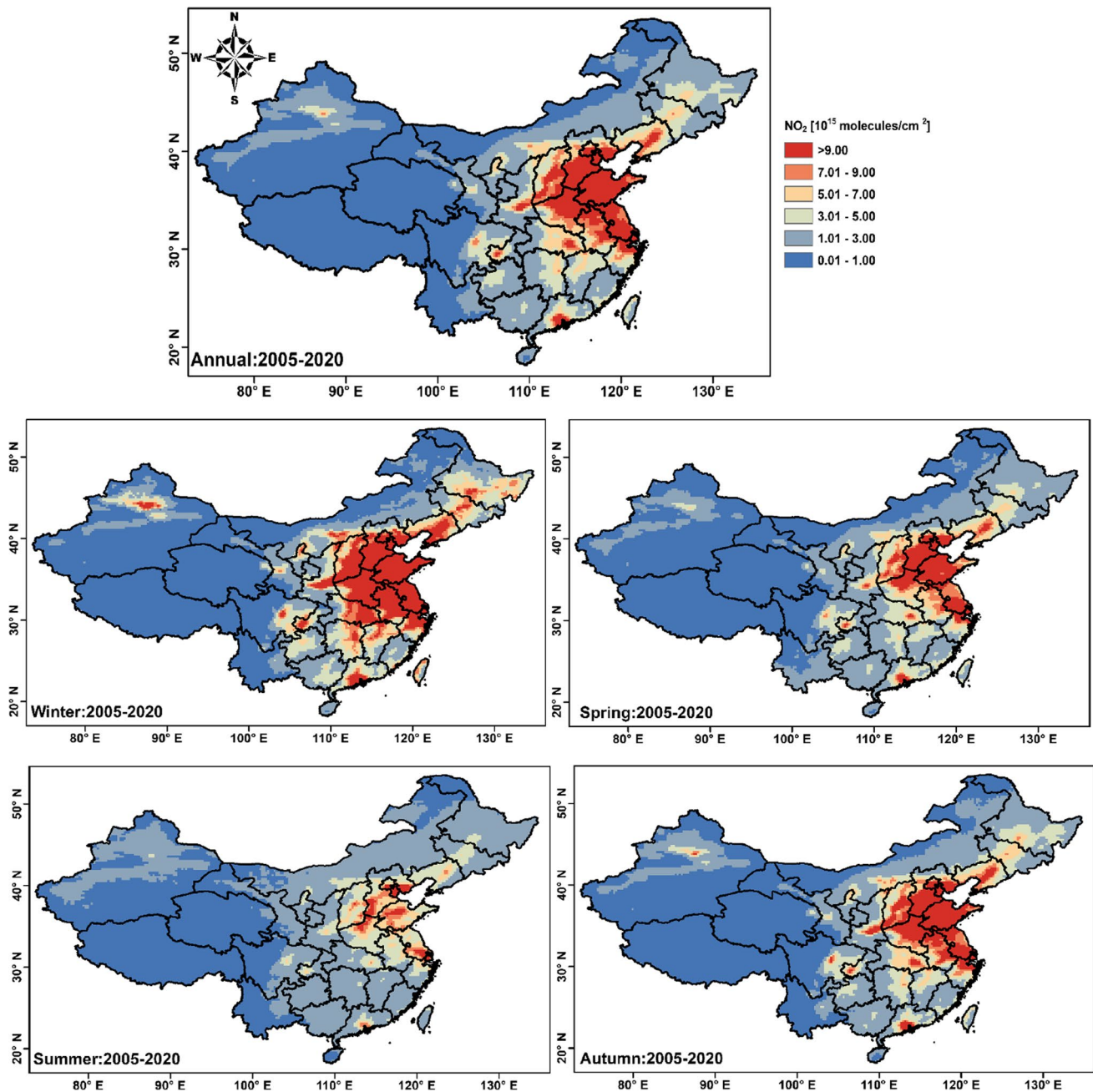


**Fig. 2** Spatial distributions of annual and seasonal mean  $\text{NO}_2$  ( $10^{15}$  molecules/cm<sup>2</sup>) obtained from Aura-based OMI over China from 2005–2020

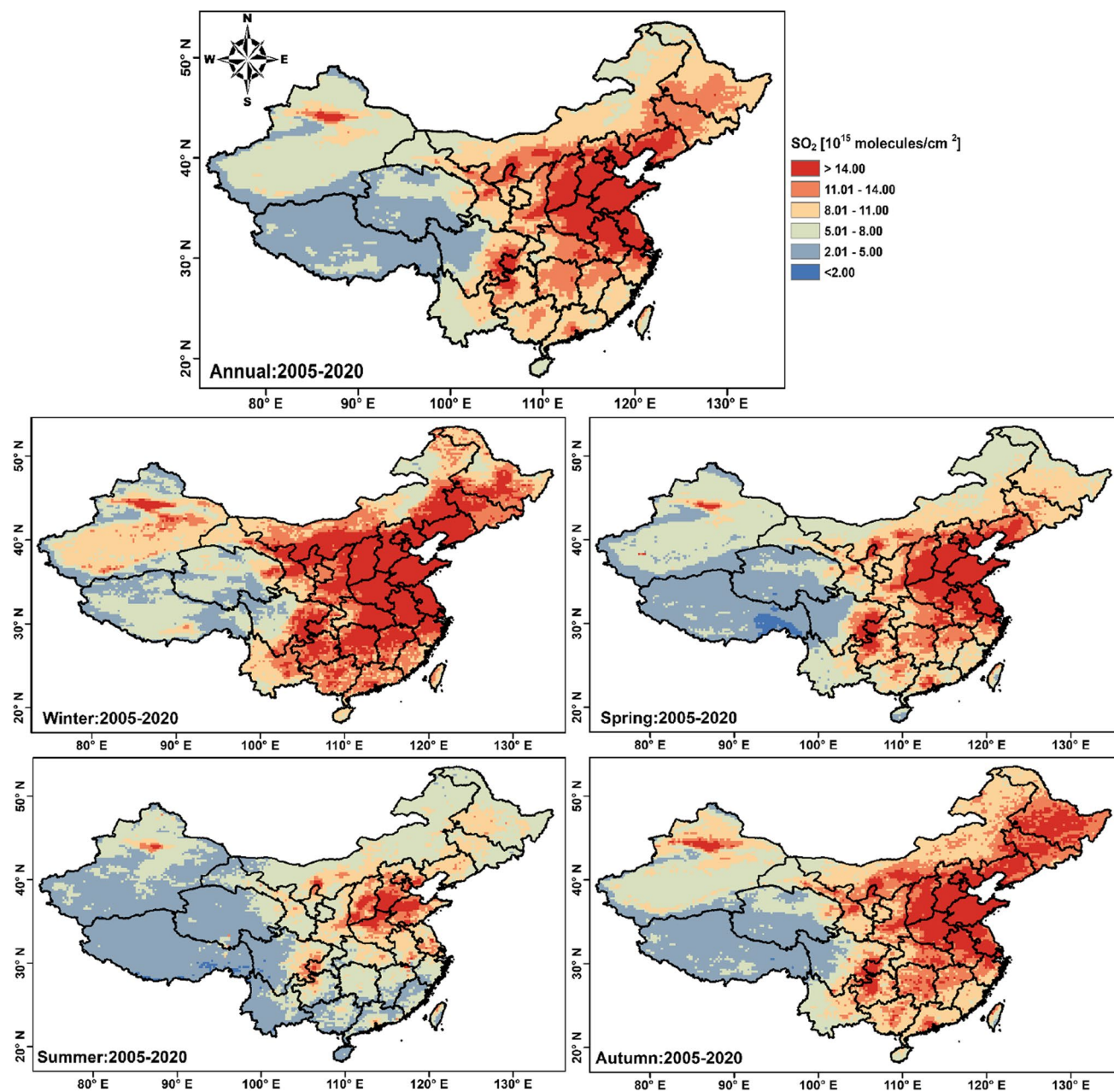


**Fig. 3** Spatial distributions of annual and seasonal mean  $\text{SO}_2$  ( $10^{15}$  molecules/ $\text{cm}^2$ ) obtained from Aura-based OMI over China from 2005 – 2020

industrialization, and urbanization have resulted in a gradual increase in  $\text{NO}_2$  levels from 2005 – 2011, whereas it has slightly decreased since 2012 due to the implementation of denitration projects in coal-fired power plants (Fig. S1). In contrast, China's  $\text{SO}_2$  levels gradually increased from 2005–2007 due to the lack of air pollution control policies during this period, whereas desulfurization projects in different industries and power plants have gradually decreased  $\text{SO}_2$  levels from 2008–2020 (Fig. S2).

In conjunction with the annual spatial distributions,  $\text{NO}_2$  and  $\text{SO}_2$  were higher across China during

winter (December–January–February) than in autumn (September–October–November), in spring (March–April–May), and summer (June–July–August) (Figs. 2 and 3), in line with the previous findings of four studies over different parts of China (Zheng et al. 2014), including 10 background and rural sites in China (Meng et al. 2010), Henan province (Zhang et al. 2017), Inner Mongolia (Zheng et al. 2018), Jiangsu Province (Wang et al. 2021a), Shanghai and Chongming Eco-Island (Xue et al. 2020). It is important to mention that the wide spatial distribution of high  $\text{SO}_2$  across China is evident compared to that of  $\text{NO}_2$ . Winter in China is expected to be characterized

by significant anthropogenic emissions, including coal-burning for winter room heating and favorable meteorological conditions (cold temperature and dry humid), resulting in higher levels of  $\text{NO}_2$  ( $> 7 \times 10^{15}$  molecules/cm<sup>2</sup>) and  $\text{SO}_2$  ( $> 11 \times 10^{15}$  molecules/cm<sup>2</sup>) in most regions, including the central, eastern, north, northeast, northwestern, south, and southwest. It is notable that in China, both December and January exhibit relatively higher levels of  $\text{NO}_2$  and  $\text{SO}_2$  in winter as compared to February (Figs. S3–S4). China experiences a smaller spatial hotspot for  $\text{NO}_2$  and  $\text{SO}_2$  in the spring compared to the winter season, which can be attributed to a decrease in coal combustion and unfavorable meteorological conditions. In particular, the month of March exhibits comparatively higher  $\text{NO}_2$  and  $\text{SO}_2$  as compared to April and May (Figs. S3–S4). In China, plenty of precipitation (i.e. wet deposition) may result in lower levels of  $\text{NO}_2$  and  $\text{SO}_2$  in summer season, in line with the findings of Zheng et al. (2018) in Inner Mongolia and Wang et al. (2021b) in Jiangsu province. In particular, the month of June exhibits comparatively higher levels of  $\text{NO}_2$  and  $\text{SO}_2$  in China as compared to July and August. In autumn and winter, the spatial hotspots for  $\text{NO}_2$  and  $\text{SO}_2$  are gradually increased across China due to the falling temperatures (Gao et al. 2022). The month of October and November exhibits comparatively higher levels of  $\text{NO}_2$  and  $\text{SO}_2$  in China than in September.

### Characterization of polluted provinces using $\text{NO}_2$ and $\text{SO}_2$

Significant annual and seasonal variations in  $\text{NO}_2$  and  $\text{SO}_2$  over 33 Chinese provinces are evident from 2005–2020 (Figs. S5–S6). In 33 Chinese provinces (Fig. 4), the 16-year

annual average  $\text{NO}_2$  varied from 0.38 to 16.86 ( $10^{15}$  molecules/cm<sup>2</sup>), with the Tianjin province identified as the topmost extremely polluted province and the Tibet as relatively less polluted. Notably, a total of 8, 18, and 7 provinces fall within the category of extremely polluted, highly polluted, and relatively less polluted provinces respectively. In particular, the 8 extremely polluted provinces in China have extreme levels of  $\text{NO}_2$  ( $10^{15}$  molecules/cm<sup>2</sup>) such as Tianjin ( $16.86 \pm 2.28$ ), Shanghai ( $15.24 \pm 2.53$ ), Shandong ( $13.04 \pm 2.35$ ), Jiangsu ( $12.02 \pm 1.61$ ), Beijing ( $11.96 \pm 1.72$ ), Hebei ( $10.92 \pm 1.90$ ), Hong Kong ( $9.91 \pm 2.44$ ), and Henan ( $9.75 \pm 1.99$ ) (Fig. 4). The 18 highly polluted provinces in China, including Macao, Anhui, Shanxi, Zhejiang, Liaoning, Hubei, Guangdong, Shaanxi, Jiangxi, Chongqing, Hunan, Jilin, Heilongjiang, Ningxia, Fujian, Guizhou, and Guangxi. China's 7 least polluted provinces include Sichuan, Inner Mongolia, Hainan, Gansu, Yunnan, Xinjiang, Qinghai, and Tibet. Seasonally, 33 Chinese provinces experience elevated levels of  $\text{NO}_2$  pollution during winter, followed by autumn, spring, and summer. Particularly, in winter, a total of 8, 13, and 12 provinces fall in the category of less polluted (Sichuan, Inner Mongolia, Hainan, Gansu, Yunnan, Xinjiang, Qinghai, Tibet), highly polluted (Liaoning, Hubei, Guangdong, Jiangxi, Hunan, Shaanxi, Heilongjiang, Chongqing, Jilin, Ningxia, Fujian, Guizhou, Guangxi), and extremely polluted (Tianjin, Shandong, Shanghai, Jiangsu, Macao, Hebei, Henan, Beijing, Hong Kong, Anhui, Shanxi, Zhejiang) respectively (Fig. 5). In spring, a total of 8, 19, and 6 provinces fall in the category of less polluted (Sichuan, Inner Mongolia, Hainan, Yunnan, Gansu, Xinjiang, Qinghai, Tibet), highly

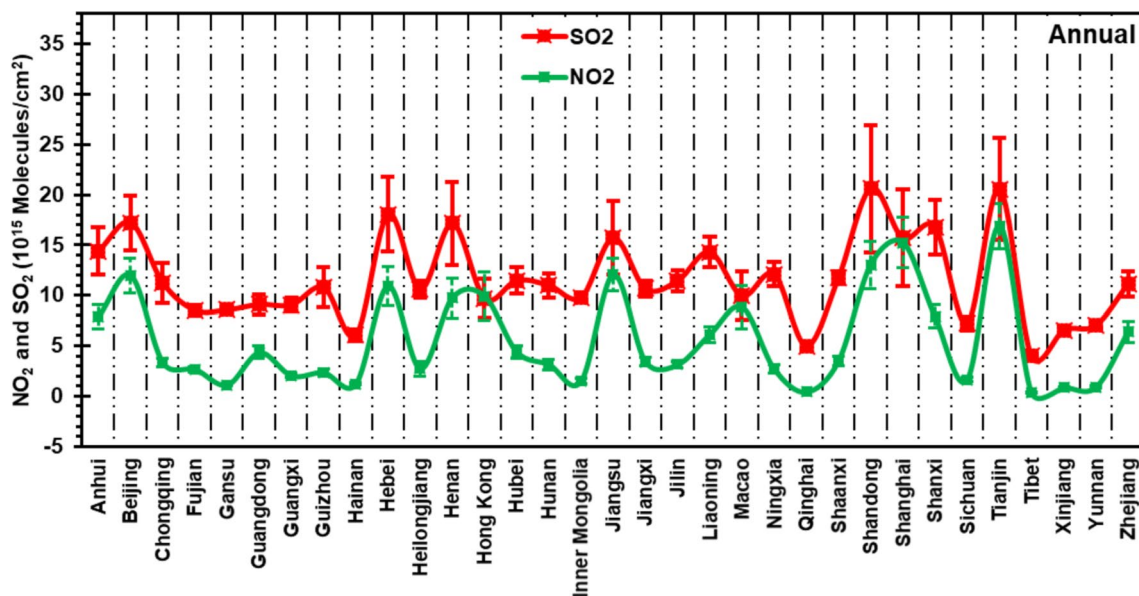


**Fig. 4** Variation per province, in annual mean  $\text{NO}_2$  and  $\text{SO}_2$  ( $10^{15}$  molecules/cm<sup>2</sup>) was obtained from Aura-based OMI over 33 provinces of China for the period 2005–2020. The error bar indicates the standard deviation of  $\text{NO}_2$  and  $\text{SO}_2$

polluted (Hong Kong, Henan, Shanxi, Anhui, Liaoning, Zhejiang, Macao, Guangdong, Hubei, Shaanxi, Chongqing, Jilin, Jiangxi, Fujian, Hunan, Ningxia, Guizhou, Guangxi, Heilongjiang), and extremely polluted (Shanghai, Tianjin, Beijing, Jiangsu, Shandong, Hebei) respectively (Fig. 6). In summer, a total of 12, 20, and 1 provinces fall in the category of less polluted (Hunan, Guizhou, Heilongjiang, Inner Mongolia, Guangxi, Sichuan, Gansu, Xinjiang, Hainan, Yunnan, Qinghai, Tibet), highly polluted (Shanghai, Beijing,

Shandong, Jiangsu, Hebei, Hong Kong, Henan, Shanxi, Anhui, Liaoning, Zhejiang, Macao, Guangdong, Hubei, Chongqing, Shaanxi, Jilin, Ningxia, Jiangxi) and extremely polluted (Tianjin:  $10.16 \pm 1.80$ ) respectively (Fig. 7). In autumn, a total of 9, 15, and 6 provinces fall in the category of less polluted (Guangxi, Sichuan, Inner Mongolia, Hainan, Gansu, Xinjiang, Yunnan, Qinghai, Tibet), highly polluted (Shanxi, Anhui, Zhejiang, Liaoning, Hubei, Guangdong, Shaanxi, Jiangxi, Chongqing, Jilin, Hunan, Ningxia, Fujian,

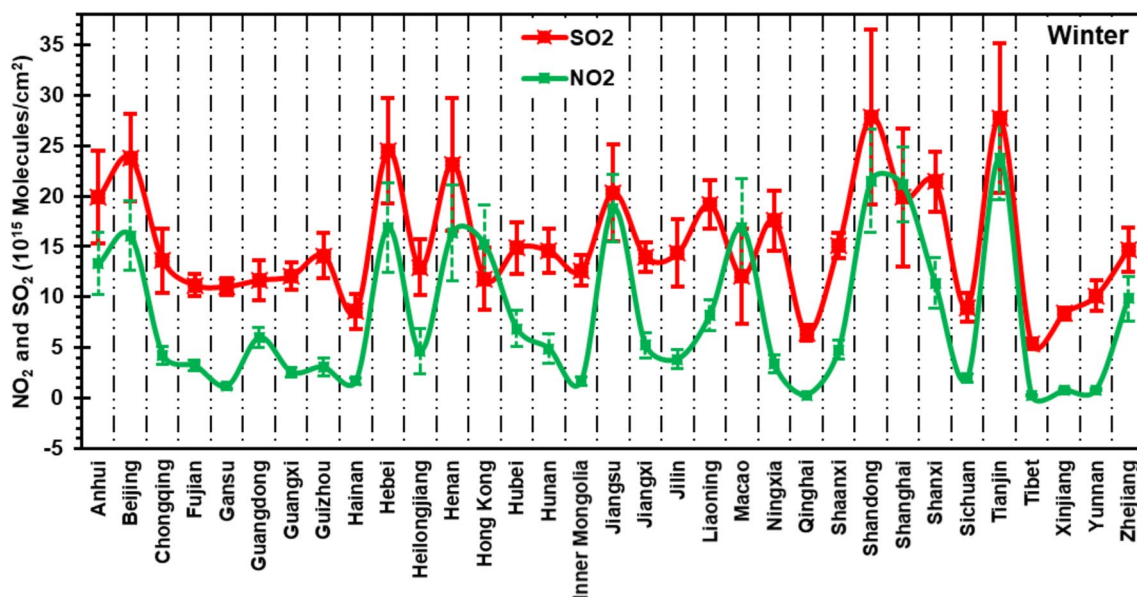


Fig. 5 Same as Fig. 4 but for wintertime NO<sub>2</sub> and SO<sub>2</sub> (10<sup>15</sup> molecules/cm<sup>2</sup>)

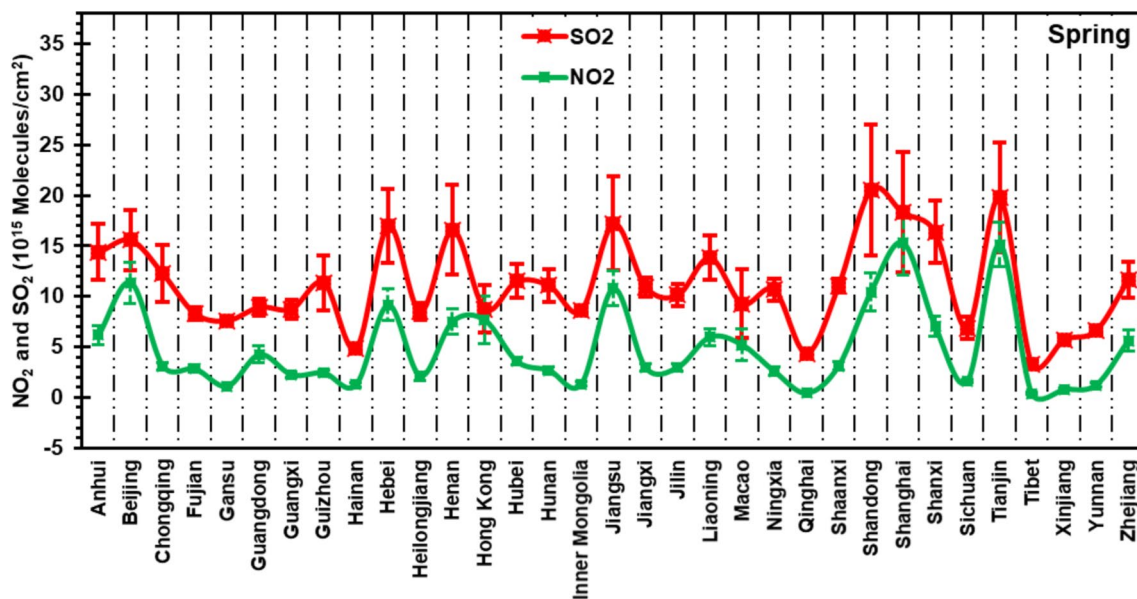


Fig. 6 Same as Fig. 4 but for springtime NO<sub>2</sub> and SO<sub>2</sub> (10<sup>15</sup> molecules/cm<sup>2</sup>)

Heilongjiang, Guizhou), and extremely polluted (Tianjin, Shanghai, Shandong, Beijing, Jiangsu, Hebei, Hong Kong, Macao, Henan) respectively (Fig. 8).

Furthermore, the 16-year annual averaged SO<sub>2</sub> varied from 3.96 to 20.62 (10<sup>15</sup> molecules/cm<sup>2</sup>) across 33 Chinese provinces, with the Shandong and Tianjin provinces identified as the topmost extremely polluted province and the Tibet (3.96 ± 0.25 10<sup>15</sup> molecules/cm<sup>2</sup>) as relatively clean (Fig. 4). Remarkably, a total of 10, 15, and 8 provinces fall within the

category of extremely polluted, highly polluted, and relatively less polluted provinces. In particular, the 10 extremely polluted provinces (e.g., Shandong, Tianjin, Hebei, Beijing, Henan, Shanxi, Jiangsu, Shanghai, Anhui, and Liaoning) in China have extreme (20.62 – 14.30 10<sup>15</sup> molecules/cm<sup>2</sup>) levels of SO<sub>2</sub> (Fig. 4). The SO<sub>2</sub> was observed highly polluted in China’s 15 provinces (Ningxia, Shaanxi, Hubei, Jilin, Chongqing, Zhejiang, Hunan, Guizhou, Jiangxi, Heilongjiang, Macao, Inner Mongolia, Hong Kong, Guangdong,

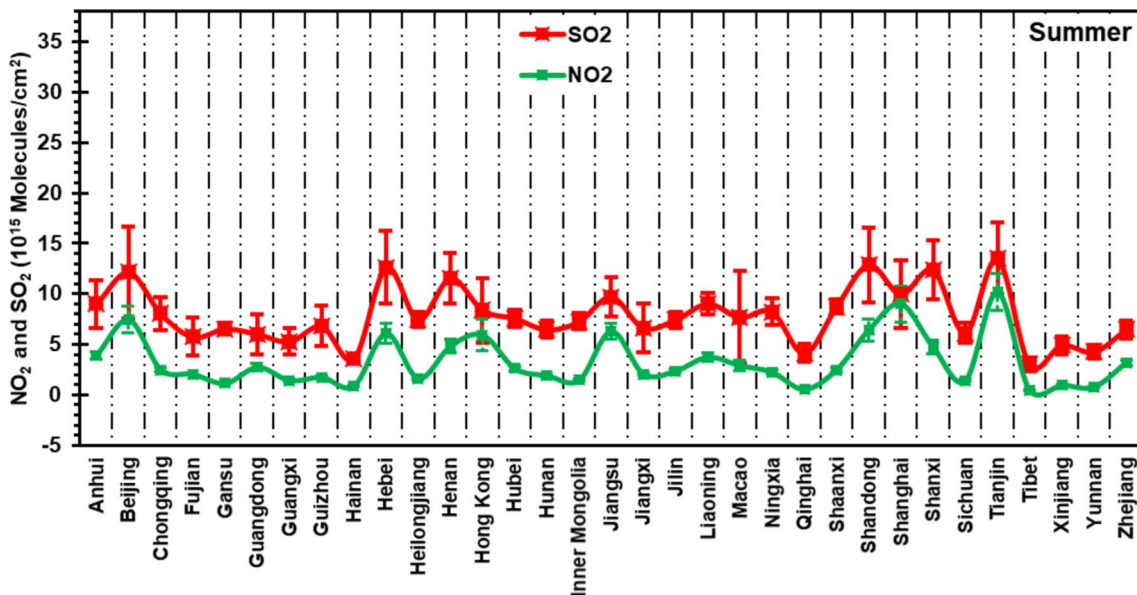


Fig. 7 Same as Fig. 4 but for summertime NO<sub>2</sub> and SO<sub>2</sub> (10<sup>15</sup> molecules/cm<sup>2</sup>)

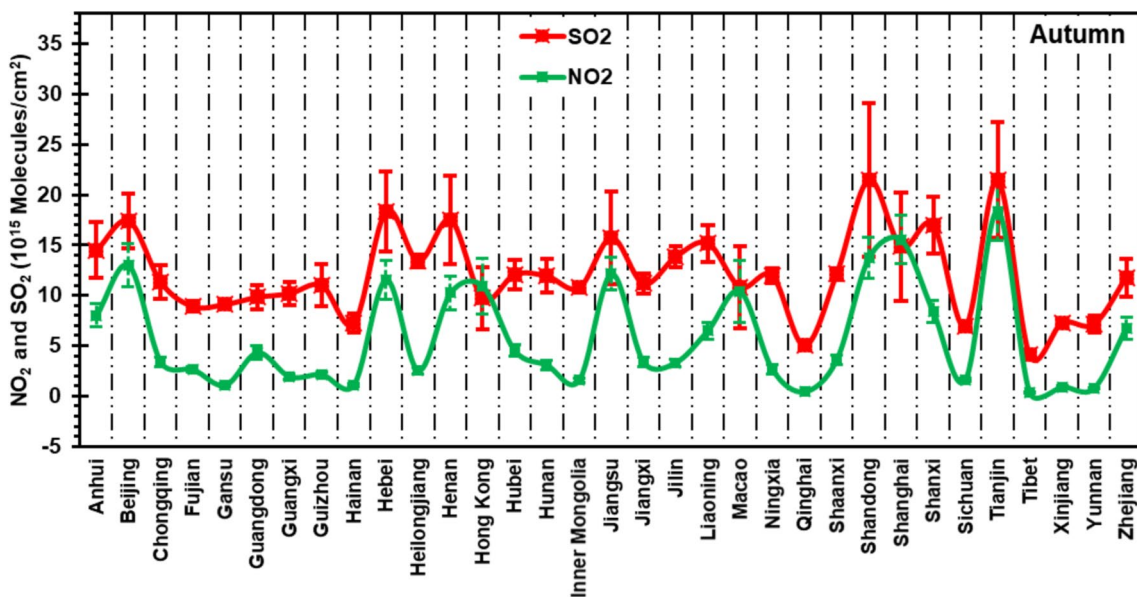


Fig. 8 Same as Fig. 4 but for autumn NO<sub>2</sub> and SO<sub>2</sub> (10<sup>15</sup> molecules/cm<sup>2</sup>)

and Guangxi). China's 8 least polluted provinces are Gansu, Fujian, Sichuan, Yunnan, Xinjiang, Hainan, and Tibet (Fig. 4). In a similar fashion to seasonal  $\text{NO}_2$ , 33 Chinese provinces experience elevated levels of  $\text{SO}_2$  pollution levels during winter, followed by autumn, spring, and summer. Particularly, in winter, a total of 5, 11, and 17 provinces fall in the category of less polluted (Sichuan, Hainan, Xinjiang, Qinghai, Tibet), highly polluted (Jiangxi, Chongqing, Heilongjiang, Inner Mongolia, Macao, Guangxi, Hong Kong, Guangdong, Fujian, Gansu, Yunnan), and extremely polluted (Shandong, Tianjin, Hebei, Beijing, Henan, Shanxi, Jiangsu, Anhui, Shanghai, Liaoning, Ningxia, Shaanxi, Hubei, Zhejiang, Hunan, Jilin, and Guizhou) respectively (Fig. 5). In spring, a total of 13, 11, and 9 provinces fall in the category of less polluted (Guangdong, Hong Kong, Guangxi, Inner Mongolia, Heilongjiang, Fujian, Gansu, Sichuan, Yunnan, Xinjiang, Hainan, Qinghai, Tibet), highly polluted provinces (Liaoning, Chongqing, Zhejiang, Hubei, Guizhou, Hunan, Shaanxi, Jiangxi, Ningxia, Jilin, Macao), and extremely polluted (Shandong, Tianjin, Shanghai, Jiangsu, Hebei, Henan, Shanxi, Beijing, Anhui) respectively (Fig. 6). In summer, a total of 24 and 9 provinces fall in the category of less polluted (Anhui, Shaanxi, Hong Kong, Ningxia, Chongqing, Macao, Hubei, Jilin, Heilongjiang, Inner Mongolia, Guizhou, Jiangxi, Gansu, Hunan, Zhejiang, Sichuan, Guangdong, Fujian, Guangxi, Xinjiang, Yunnan, Qinghai, Hainan, Tibet), and highly polluted provinces (Tianjin, Shandong, Hebei, Shanxi, Beijing, Henan, Shanghai, Jiangsu, Liaoning) respectively while extremely polluted is nil (Fig. 7). In autumn, a total of 7, 16, and 10 provinces fall in the category of less polluted (Fujian, Xinjiang, Hainan, Yunnan,

Sichuan, Qinghai, Tibet), highly polluted (Jilin, Heilongjiang, Shaanxi, Hubei, Ningxia, Hunan, Zhejiang, Chongqing, Jiangxi, Guizhou, Macao, Inner Mongolia, Guangxi, Guangdong, Hong Kong, Gansu), and extremely polluted (Shandong, Tianjin, Hebei, Henan, Beijing, Shanxi, Jiangsu, Liaoning, Shanghai, Anhui) respectively (Fig. 8).

### Ratio of $\text{SO}_2/\text{NO}_2$ at provincial level

By using the  $\text{SO}_2/\text{NO}_2$  ratio, we can discern whether they come from mobile sources (road traffic emissions) or point sources (industrial activities) (Abdul Halim et al. 2018; Aneja et al. 2001; Nirel and Dayan 2001). A high value of the  $\text{SO}_2/\text{NO}_2$  ratio ( $> 0.60$ ) indicates significant contributions from industrial activities over land (Wang et al. 2021a). The present study excluded five provinces (Gansu, Inner Mongolia, Qinghai, Tibet, Xinjiang, and Yunnan) from  $\text{SO}_2/\text{NO}_2$  ratio calculations due to their low level of  $\text{NO}_2$ . The results show significant annual and seasonal variations in  $\text{SO}_2/\text{NO}_2$  ratio over 33 Chinese provinces (Figs. 9 and S7). Annually, the  $\text{SO}_2/\text{NO}_2$  ratio over 27 Chinese provinces was ranged from 0.67 to 7.15 during 2005–2008, indicating more  $\text{SO}_2$  emissions than  $\text{NO}_2$  from point sources. Afterward, the ratio gradually drops from 2009 over most Chinese provinces ( $\text{SO}_2/\text{NO}_2$ : 0.69–5.90) except for Hong Kong and Macao (Fig. S7). The installation of the fuel gas desulfurization (FGD) device in the industry in 2007 (Zhang et al. 2017) may reduce  $\text{SO}_2$  emissions over land (Wang et al. 2021a). The 16-year annual mean  $\text{SO}_2/\text{NO}_2$  ratio ranged from 1.02 to 4.98 across 27 Chinese provinces, indicating comparatively higher  $\text{SO}_2$  emissions than  $\text{NO}_2$  from point sources (e.g., industries) (Fig. 9). Across

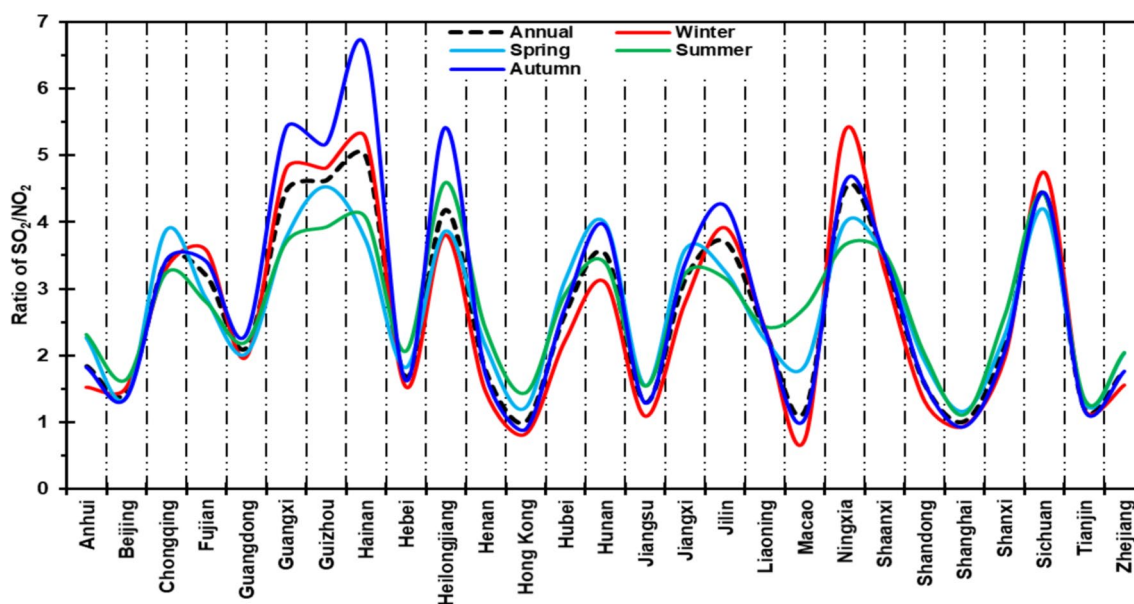


Fig. 9 Variation per province, annual and seasonal mean ratio of  $\text{SO}_2/\text{NO}_2$  over 33 provinces of China for the period 2005–2020

**Table 1** Estimation of Provincial trends of NO<sub>2</sub> using OLS regression method with the Mann–Kendall test using monthly data over China from 2005 to 2020. Here, 1st segment = before breakpoint and 2nd segment = after breakpoint. Trend values in Bold = significant (at the 95% confident interval) and non-bold = insignificant trend

Province	Breakpoint	Mean NO <sub>2</sub> (1st segment)	Trend (1st Segment) (% change)	Mean NO <sub>2</sub> (2nd segment)	Trend (2nd segment) (% change)
Anhui	2014	8.51	<b>0.29 (34%)</b>	6.84	0.02 (2%)
Beijing	2013	13.11	<b>0.47 (32%)</b>	10.47	<b>-0.32 (-22%)</b>
Chongqing	2015	3.35	<b>0.10 (33%)</b>	3.31	<b>0.19 (29%)</b>
Fujian	2014	2.73	<b>0.05 (20%)</b>	2.61	<b>0.06 (15%)</b>
Gansu	2010	1.00	<b>0.03 (20%)</b>	1.21	-0.01 (-12%)
Guangdong	No break	4.34	<b>-0.10 (-37%)</b>		
Guangxi	2014	2.09	<b>0.04 (17%)</b>	1.96	<b>0.06 (19%)</b>
Guizhou	2014	2.50	<b>0.06 (23%)</b>	2.12	<b>0.07 (20%)</b>
Hainan	No break	1.23	-0.01 (-8%)		
Hebei	2013	11.77	<b>0.91 (70%)</b>	9.83	<b>-0.42 (-30%)</b>
Heilongjiang	2009	2.18	<b>0.35 (81%)</b>	3.00	<b>-0.19 (-69%)</b>
Henan	2014	10.88	<b>0.52 (48%)</b>	7.88	<b>-0.17 (-13%)</b>
Hong Kong	2008	13.38	0.33 (10%)	8.75	<b>-0.35 (-52%)</b>
Hubei	2014	4.62	<b>0.21 (46%)</b>	4.07	0.03 (4%)
Hunan	No break	3.16	-0.02 (-12%)		
Inner Mongolia	2013	1.53	0.22 (128%)	1.48	-0.17 (-81%)
Jiangsu	No break	12.02	0.00005 (0%)		
Jiangxi		3.44	0.01 (5%)		
Jilin	2013	3.15	<b>0.36 (102%)</b>	3.11	<b>-0.17 (-38%)</b>
Liaoning		6.13	<b>-0.42 (-110%)</b>		
Macao	2013	10.33	<b>0.13 (11%)</b>	6.90	<b>-0.02 (-2%)</b>
Ningxia	2010	2.44	<b>0.06 (14%)</b>	2.91	<b>-0.11 (-37%)</b>
Qinghai	2013	0.40	<b>0.02 (44%)</b>	0.47	<b>-0.01 (-14%)</b>
Shaanxi	2013	3.50	<b>0.21 (53%)</b>	3.48	-0.01 (-3%)
Shandong	2014	14.27	<b>0.70 (49%)</b>	10.98	<b>-0.42 (-23%)</b>
Shanghai		15.24	<b>-0.51 (-53%)</b>		
Shanxi	2013	8.49	<b>0.44 (47%)</b>	7.12	<b>-0.15 (-15%)</b>
Sichuan	2014	1.65	<b>0.08 (49%)</b>	1.65	<b>0.02 (7%)</b>
Tianjin	2009	16.44	0.40 (12%)	17.06	<b>-0.76 (-49%)</b>
Tibet	2016	0.37	<b>0.05 (139%)</b>	0.40	-0.01 (-18%)
Xinjiang	2015	0.84	<b>0.01 (17%)</b>	0.90	<b>-0.01 (-9%)</b>
Yunnan	2010	0.82	<b>0.03 (20%)</b>	0.95	<b>-0.01 (-15%)</b>
Zhejiang		6.37	<b>-0.15 (-37%)</b>		

27 Chinese provinces, SO<sub>2</sub> emissions were relatively higher than NO<sub>2</sub> in all seasons such as autumn (0.89–6.61) followed by in winter (0.74–5.37), summer (1.11–4.59), and spring (1.16–4.53) (Fig. 9).

## NO<sub>2</sub> and SO<sub>2</sub> trend

To better understand the variability in NO<sub>2</sub> and SO<sub>2</sub> across 33 provinces in China, we calculate the NO<sub>2</sub> and SO<sub>2</sub> trend using the ordinary least square (OLS) regression method, and the significance of the trend is determined using the Man-Kendall trend test applied to seasonal-adjusted time series. For the entire analysis period, the increased and decreased trends for NO<sub>2</sub> and SO<sub>2</sub> are observed in 33

provinces of China (not shown). The annual trend analysis revealed that NO<sub>2</sub> decreased over 19 provinces and increased over 14 provinces whilst SO<sub>2</sub> decreased over 26 provinces and increased over 7 provinces, respectively. The highest decrease of NO<sub>2</sub> was observed in Shanghai (0.51/year) whilst the highest decrease of SO<sub>2</sub> was observed in Shandong (1.24). Furthermore, NO<sub>2</sub> and SO<sub>2</sub> trend was performed by segmenting the data into two categories: 1st segment (before breakpoint) and 2nd segment (after breakpoint), as shown in Tables 1, 2, 3 and 4. Furthermore, the study applied Theil-Sen's Slope and bootstrapping methods to test how robust the results were obtained using OLS regression and the trend is shown in Tables 2 and 4. In general, trends before breakpoints are higher than the same after

**Table 2** Estimation of Provincial trends of NO<sub>2</sub> using the Theil–Sen's and bootstrapping approaches with the Mann–Kendall test using monthly data over China from 2005 to 2020. Here, 1st segment = before breakpoint and 2nd segment = after breakpoint. Trend values in Bold = significant (at the 95% confident interval) and non-bold = insignificant trend

Province	Breakpoint	Mean NO <sub>2</sub> (1st segment)	Trend (1st Segment) (% change)	Mean NO <sub>2</sub> (2nd segment)	Trend (2nd segment) (% change)
Anhui	2014	8.51	<b>0.09 (11%)</b>	6.84	0.05 (5%)
Beijing	2013	13.11	<b>0.18 (12%)</b>	10.47	<b>-0.39 (-26%)</b>
Chongqing	2015	3.35	<b>0.05 (18%)</b>	3.31	<b>0.11 (17%)</b>
Fujian	2014	2.73	<b>0.03 (12%)</b>	2.61	<b>0.06 (14%)</b>
Gansu	2010	1.00	<b>0.04 (23%)</b>	1.21	-0.001 (-1%)
Guangdong	No break	4.34	<b>-0.09 (-32%)</b>		
Guangxi	2014	2.09	<b>0.03 (14%)</b>	1.96	<b>0.04 (13%)</b>
Guizhou	2014	2.50	<b>0.02 (10%)</b>	2.12	<b>0.03 (9%)</b>
Hainan	No break	1.23	-0.001 (-1%)		
Hebei	2013	11.77	<b>0.52 (40%)</b>	9.83	<b>-0.37 (-26%)</b>
Heilongjiang	2009	2.18	<b>0.13 (30%)</b>	3.00	<b>-0.08 (-29%)</b>
Henan	2014	10.88	<b>0.18 (16%)</b>	7.88	<b>-0.10 (-8%)</b>
Hong Kong	2008	13.38	-0.67 (-20%)	8.75	<b>-0.28 (-41%)</b>
Hubei	2014	4.62	<b>0.08 (17%)</b>	4.07	0.05 (8%)
Hunan	No break	3.16	-0.02 (-8%)		
Inner Mongolia	2013	1.53	0.07 (44%)	1.48	-0.13 (-60%)
Jiangsu	No break	12.02	0.01 (1%)		
Jiangxi		3.44	-0.004 (-2%)		
Jilin	2013	3.15	<b>0.21 (60%)</b>	3.11	<b>-0.09 (-20%)</b>
Liaoning		6.13	<b>-0.25 (-64%)</b>		
Macao	2013	10.33	<b>0.08 (7%)</b>	6.90	<b>-0.01 (-1%)</b>
Ningxia	2010	2.44	<b>0.06 (15%)</b>	2.91	<b>-0.04 (-15%)</b>
Qinghai	2013	0.40	<b>0.02 (48%)</b>	0.47	<b>-0.01 (-9%)</b>
Shaanxi	2013	3.50	<b>0.14 (36%)</b>	3.48	0.01 (3%)
Shandong	2014	14.27	<b>0.36 (25%)</b>	10.98	<b>-0.21</b>
Shanghai		15.24	<b>-0.41 (-43%)</b>		
Shanxi	2013	8.49	<b>0.28 (30%)</b>	7.12	<b>-0.09 (-12%)</b>
Sichuan	2014	1.65	<b>0.05 (30%)</b>	1.65	<b>0.01 (4%)</b>
Tianjin	2009	16.44	0.63 (19%)	17.06	<b>-0.71 (-46%)</b>
Tibet	2016	0.37	<b>0.03 (95%)</b>	0.40	0.01 (13%)
Xinjiang	2015	0.84	<b>0.01 (16%)</b>	0.90	<b>-0.02 (-11%)</b>
Yunnan	2010	0.82	<b>0.03 (20%)</b>	0.95	<b>-0.01 (-14%)</b>
Zhejiang		6.37	<b>-0.08 (-20%)</b>		

breakpoints with a few exceptions for example Heilongjiang, Shaanxi, Qinghai, Ningxia, Yunnan, Xinjiang, and Tibet have higher trends after the breakpoint than before the breakpoint (Table 1). For SO<sub>2</sub>, many provinces have no breakpoints while for NO<sub>2</sub> the number of provinces with no break is only a few. It is noteworthy that all three methods tend to provide comparable magnitudes for the estimates of trends and significance levels as shown in Tables 1–4.

### Measuring the effectiveness of APCP on NO<sub>2</sub> and SO<sub>2</sub>

The effectiveness of air pollution control policies (APCP) on NO<sub>2</sub> and SO<sub>2</sub> during the 11th, 12th, and 13th Five-Year Plan (FYP) periods was measured. Therefore, NO<sub>2</sub> and SO<sub>2</sub>

trends were calculated using the OLS regression technique for 2006–2010 (11th FYP), 2011–2015 (12th FYP), and 2016–2020 (13th FYP) (Figs. 10 and S8–S9). NO<sub>2</sub> trends over 33 Chinese provinces were noticeably decreasing during the 12th FYP period, following the 13th FYP period and 11th FYP period. During the 12th FYP period, the largest decrease in NO<sub>2</sub> was seen in Hunan (-66%) (Fig. 10). The significant reduction in NO<sub>2</sub> is due to denitration facilities installed in coal-fired power plants and in major industrial sectors, as well as controls on NO<sub>x</sub> emissions from vehicles and ships. During the 13th FYP period, the largest decrease in NO<sub>2</sub> was seen in Heilongjiang (-52%) compared to other provinces (Fig. 10). China experienced no significant reduction in NO<sub>2</sub> during the 11th FYP period because NO<sub>2</sub>

**Table 3** Estimation of Provincial trends of SO<sub>2</sub> using OLS regression method with the Mann–Kendall test using monthly data over China from 2005 to 2020. Here, 1st segment = before breakpoint and 2nd segment = after breakpoint. Trend values in Bold = significant (at the 95% confident interval) and non-bold = insignificant trend

Province	Breakpoint	Mean SO <sub>2</sub> (1st segment)	Trend (1st Segment) (% change)	Mean SO <sub>2</sub> (2nd segment)	Trend (2nd segment) (% change)
Anhui	No break	14.41	<b>-0.45 (-50%)</b>		
Beijing	No break	17.22	<b>-0.51 (-47%)</b>		
Chongqing	No break	11.22	<b>-0.37 (-52%)</b>		
Fujian	No break	8.52	0.02 (4%)		
Gansu	No break	8.57	0.01 (2%)		
Guangdong	No break	9.10	<b>-0.12 (-20%)</b>		
Guangxi	No break	9.06	<b>-0.09 (-16%)</b>		
Guizhou	No break	10.78	<b>-0.35 (-51%)</b>		
Hainan	No break	6.05	0.01 (1%)		
Hebei	No break	18.05	<b>-0.74 (-65%)</b>		
Heilongjiang	2008	11.15	0.59 (21%)	10.41	<b>0.11 (13%)</b>
Henan	2008	22.64	<b>2.21 (39%)</b>	15.31	<b>-0.68 (-54%)</b>
Hong Kong	No break	9.69	<b>-0.22 (-35%)</b>		
Hubei	No break	11.47	<b>-0.24 (-33%)</b>		
Hunan	No break	10.99	<b>-0.20 (-29%)</b>		
Inner Mongolia	2008	9.90	1.03 (42%)	9.75	<b>-0.53 (-66%)</b>
Jiangsu	No break	15.70	<b>-0.08 (-8%)</b>		
Jiangxi	2017	10.75	<b>-0.17 (-20%)</b>	10.23	<b>-1.21 (-35%)</b>
Jilin	2008	12.39	<b>0.65 (21%)</b>	11.13	<b>-0.19 (-21%)</b>
Liaoning	No break	14.30	<b>-0.25 (-28%)</b>		
Macao	2017	10.19	-0.02 (-2%)	8.91	<b>-1.04 (-35%)</b>
Ningxia	2010	11.85	0.11 (6%)	12.24	<b>-0.42 (-24%)</b>
Qinghai	No break	5.00	<b>0.01 (5%)</b>		
Shaanxi	No break	11.74	<b>-0.10 (-14%)</b>		
Shandong	2010	25.80	<b>-1.82 (-42%)</b>	17.52	<b>-1.68 (-96%)</b>
Shanghai	2008	23.26	-0.95 (-16%)	13.17	<b>-0.33 (-30%)</b>
Shanxi	No break	16.77	<b>-0.54 (-51%)</b>		
Sichuan	No break	7.21	<b>-0.13 (-28%)</b>		
Tianjin	2008	27.44	<b>1.30 (19%)</b>	18.26	<b>-0.83 (-55%)</b>
Tibet	No break	3.96	<b>0.04 (15%)</b>		
Xinjiang	No break	6.57	<b>0.01 (4%)</b>		
Yunnan	No break	7.03	-0.06 (-13%)		
Zhejiang	2008	12.93	0.58 (18%)	10.52	-0.05 (-6%)

reduction policies did not exist during that time. However, only seven provinces (Hong Kong, Macao, Guangdong, Shanghai, Zhejiang, Fujian, and Hainan) have experienced significant decreases in NO<sub>2</sub>, which may be caused by implementing the total emission controls policy for key industrial pollution sources and strengthening the prevention and control of vehicle pollution, improving gasoline quality and efficiency, as well as favorable meteorological conditions.

Furthermore, there was a noticeably decreased trend in SO<sub>2</sub> levels across 33 Chinese provinces during the 11th FYP period compared to the 12th FYP and 13th FYP periods (Figs. 10 and S8–S9). During the 11th FYP period, the largest decrease in SO<sub>2</sub> was seen in Macao–Hong Kong (-74%) (Fig. S8). During the 12th FYP period, the largest decrease in SO<sub>2</sub> was seen in Macao (-65%) (Fig. 10). During the 13th FYP period, the

largest decrease in SO<sub>2</sub> was seen in Shanxi (-26%) (Fig. S9). SO<sub>2</sub> levels declined significantly during the 11th, 12th, and 13th FYP periods as a result of desulfurization projects implemented at coal-fired power plants and major industrial sectors, as well as the prevention and control of urban air pollution.

## Discussion

In this study, long-term spatiotemporal distributions and variations, characterization and ranking of polluted provinces, SO<sub>2</sub>/NO<sub>2</sub> ratio calculation for source identification, and trends in NO<sub>2</sub> and SO<sub>2</sub> pollution over China were investigated using data from Aura-based OMI sensor from

**Table 4** Estimation of Provincial trends of SO<sub>2</sub> using the Theil-Sen's and bootstrapping approaches with the Mann–Kendall test using monthly data over China from 2005 to 2020. Here, 1st segment = before breakpoint and 2nd segment = after breakpoint. Trend values in Bold = significant (at the 95% confident interval) and non-bold = insignificant trend

Province	Breakpoint	Mean SO <sub>2</sub> (1st segment)	Trend (1st Segment) (% change)	Mean SO <sub>2</sub> (2nd segment)	Trend (2nd segment) (% change)
Anhui	No break	14.41	<b>-0.37 (-41%)</b>		
Beijing	No break	17.22	<b>-0.43 (-40%)</b>		
Chongqing	No break	11.22	<b>-0.31 (-44%)</b>		
Fujian	No break	8.52	0.03 (5%)		
Gansu	No break	8.57	<b>0.02 (3%)</b>		
Guangdong	No break	9.10	<b>-0.05 (-9%)</b>		
Guangxi	No break	9.06	<b>-0.04 (-8%)</b>		
Guizhou	No break	10.78	<b>-0.30 (-44%)</b>		
Hainan	No break	6.05	0.01 (2%)		
Hebei	No break	18.05	<b>-0.66 (-59%)</b>		
Heilongjiang	2008	11.15	0.15 (5%)	10.41	0.04 (5%)
Henan	2008	22.64	<b>-0.20 (-4%)</b>	15.31	-0.60 (-47%)
Hong Kong	No break	9.69	<b>-0.13 (-22%)</b>		
Hubei	No break	11.47	<b>-0.18 (-26%)</b>		
Hunan	No break	10.99	<b>-0.14 (-21%)</b>		
Inner Mongolia	2008	9.90	-0.69 (-28%)	9.75	<b>-0.42 (-52%)</b>
Jiangsu	No break	15.70	<b>-0.05 (-6%)</b>		
Jiangxi	2017	10.75	<b>-0.08 (-10%)</b>	10.23	<b>-0.49 (-14%)</b>
Jilin	2008	12.39	<b>0.29 (9%)</b>	11.13	<b>-0.15 (-16%)</b>
Liaoning	No break	14.30	<b>-0.13 (-15%)</b>		
Macao	2017	10.19	-0.01 (-1%)	8.91	<b>-0.23 (-8%)</b>
Ningxia	2010	11.85	0.14 (7%)	12.24	<b>-0.32 (-26%)</b>
Qinghai	No break	5.00	<b>0.03 (9%)</b>		
Shaanxi	No break	11.74	<b>-0.08 (-12%)</b>		
Shandong	2010	25.80	<b>-1.68 (-39%)</b>	17.52	<b>-1.24 (-71%)</b>
Shanghai	2008	23.26	-1.36 (-23%)	13.17	<b>-0.32 (-29%)</b>
Shanxi	No break	16.77	<b>-0.50 (-48%)</b>		
Sichuan	No break	7.21	<b>-0.09 (-21%)</b>		
Tianjin	2008	27.44	<b>-0.56 (-8%)</b>	18.26	<b>-0.71 (-47%)</b>
Tibet	No break	3.96	<b>0.04 (15%)</b>		
Xinjiang	No break	6.57	<b>0.02 (5%)</b>		
Yunnan	No break	7.03	-0.004 (-1%)		
Zhejiang	2008	12.93	-0.13 (-4%)	10.52	-0.04 (-4%)

2005–2020. The study also quantifies the impact of the Air Pollution Control Policy (APCP) on NO<sub>2</sub> and SO<sub>2</sub> pollutants.

The long-term (2005–2020) spatiotemporal distributions of NO<sub>2</sub> and SO<sub>2</sub> show pollution hotspots across China's central (Hubei), eastern (Jiangsu, Anhui, Zhejiang), northern (Beijing, Hebei, Henan, Shandong, Shanxi, Tianjin), northeast (Liaoning, Jilin), northwestern (Urumqi), south (Guangdong, Hong Kong), and southwest (Chongqing, Sichuan) regions, which is mainly due to the rapid growth of industrialization and urbanization and dense population with maximum energy consumption. There was more NO<sub>2</sub> and SO<sub>2</sub> pollution over eastern parts of China as a result of human activity (Wang et al. 2021a). In an earlier study, it was found that several Jiangsu cities are host to many

industries and have high traffic volumes, all of which result in high levels of NO<sub>2</sub> and SO<sub>2</sub> (Song et al. 2019). Lamsal et al. (2013) reported that dense population and unsustainable anthropogenic emissions from mobile sources (e.g., traffic emissions) also contribute to high NO<sub>2</sub> pollution. A significant increase in industrial development and traffic in eastern China is another important reason for the increasing NO<sub>2</sub> (Streets et al. 2003; Wang 2004). The industry was the top source of NO<sub>2</sub> emission (39%) in China in 2010, followed by power plants (32%), traffic (25%), and residential activities (4%) (Li et al. 2017b). In addition, China is the world's third-largest emitter of SO<sub>2</sub> due to having the most coal-fired power plants (total number of coal-fired plants = 86) (Dahiya and Myllyvirta 2019). Apart from

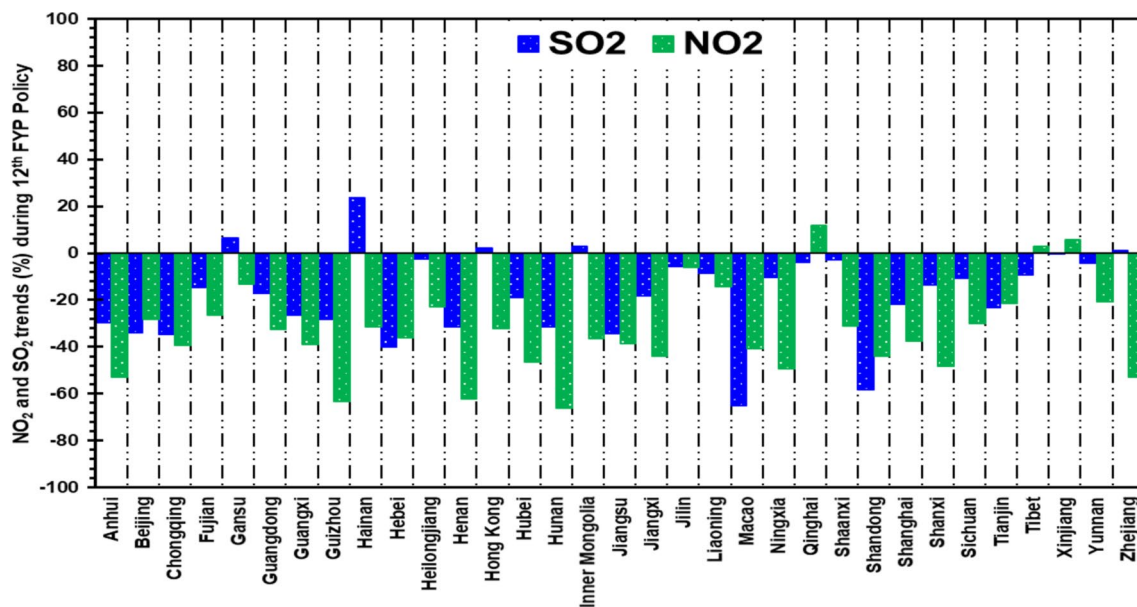


**Fig. 10** Trends in NO<sub>2</sub> and SO<sub>2</sub> over 33 provinces of China for the period 12<sup>th</sup> FYP (2011–2015). The white dots (.) represent significant trends at a 95% confidence level

these, Cheng et al. (2019) reported that the Ship Emission Control Zones of China (ECZ) in the Pearl River Delta (PRD), the Yangtze River Delta (YRD), and the Bohai Rim (Beijing-Tianjin-Hebei) is the main source of NO<sub>2</sub> and SO<sub>2</sub> levels.

Seasonally, the winter season has higher levels of NO<sub>2</sub> and SO<sub>2</sub> pollution than other seasons across China because of increased anthropogenic activities and stable atmospheric conditions (shallower boundary layer and stagnant conditions), in line with the previous findings of four studies over different parts of China (Zheng et al. 2014), including 10 background and rural sites in China (Meng et al. 2010), Henan province (Zhang et al. 2017), Inner Mongolia (Zheng et al. 2018), Beijing (He et al. 2023), Jiangsu Province (Wang et al. 2021a; Ali et al. 2023b), Shanghai and Chongming Eco-Island (Xue et al. 2020). This is attributed mainly to stable meteorological conditions, weak photochemical conversion, and coal burning for winter room heating (Qi et al. 2012; Zhang et al. 2017). In winter, the stable atmospheric conditions and low boundary layer height accumulate and slow down the NO<sub>2</sub> washing-out process in the atmosphere, resulting in high NO<sub>2</sub> in the tropospheric column (Bilal et al. 2021; Mhawish et al. 2020; Qi et al. 2012; Zhang et al. 2017). Moreover, abundant precipitation, rapid photochemical conversion, and better atmospheric diffusion during the summer season may lower the summertime NO<sub>2</sub> and SO<sub>2</sub> throughout China from 2005–2020 (Feng et al. 2001; Qi et al. 2012).

Furthermore, the 16-year annual average NO<sub>2</sub> and SO<sub>2</sub> demonstrated that Tianjin province was the topmost

extremely polluted province and Tibet the least polluted province. Several factors contribute to Tianjin's pollution, including high industrial activity and traffic emissions, as well as geographical factors (e.g., Tianjin's geographical location, with its proximity to Bohai sea and coastal areas can cause stagnant weather conditions that trap pollutants in the air), high coal consumption, and weather conditions (e.g., low wind speed and temperature inversions) (Qi et al. 2012; Zhang et al. 2017; Cai et al. 2020; Xiao et al. 2020).

In general, a total of 30 Chinese provinces demonstrated a significant decrease in NO<sub>2</sub> (6%–66%) during the 12th FYP period (2011–2015), whilst 33 Chinese provinces demonstrated a significant decrease in SO<sub>2</sub> (3%–74%) during the 11th FYP period (2006–2010) (see Figs. 10 and S8). However, several factors could be accounted for the increase and decrease in NO<sub>2</sub> and SO<sub>2</sub> across China from 2005 to 2020. For example, desulfurization projects in coal-fired power plants were implemented during the 11th Five Year Plan (FYP) period (2006–2010) and continued for the 12th FYP period (2011–2015) and 13th FYP period (2016–2020) (Li et al. 2017a; Ma et al. 2019), which overall led to decreasing trends in SO<sub>2</sub> in China. In contrast, the absence of any control policies for reducing NO<sub>2</sub> emission during the 11th Five Year Plan (FYP) period (2006–2010) (Ma et al. 2019) allowed increased NO<sub>2</sub> concentrations during that period (see Fig. S8). However, denitration facilities for coal-fired power plants and major industrial sectors were implemented during the 12th FYP period (2011–2015), which overall led to decreasing trends in NO<sub>2</sub> in China. The extremely polluted provinces

in China such as Tianjin, Shanghai, Shandong, Jiangsu, Beijing, Hebei, Hong Kong, and Henan are recommended to take preventive measures against NO<sub>2</sub> pollutants. Similarly, Shandong, Tianjin, Hebei, Beijing, Henan, Shanxi, Jiangsu, Shanghai, Anhui, and Liaoning provinces in China need to take precautions against extremely high SO<sub>2</sub> levels. Accordingly, a comprehensive strategy to reduce air pollution maybe adopted by the Chinese government, including investing in clean energy, promoting electric vehicles, enforcing strict emission standards for industries, promoting green building practices, and raising public awareness about reducing air pollution.

## Conclusions

In the current study, we aimed to identify the long-term (2005–2020) NO<sub>2</sub> and SO<sub>2</sub> pollution hotspots and emission sources in China by analyzing spatiotemporal distributions and variations, ratio SO<sub>2</sub>/NO<sub>2</sub>, characterization of polluted provinces, and trend. Our major findings are as follows:

- China's central (Hubei), eastern (Jiangsu, Anhui, Zhejiang), northern (Beijing, Hebei, Henan, Shandong, Shanxi, Tianjin), northeast (Liaoning, Jilin), northwest (Urumqi), South (Guangdong, Hong Kong), and southwest (Chongqing, Sichuan) regions were identified as hotspots of NO<sub>2</sub> and SO<sub>2</sub> pollutions that occur more frequently in winter than in autumn, spring, or summer.
- In terms of NO<sub>2</sub>, China's 8 provinces are identified as extremely polluted provinces, including Tianjin ( $16.86 \pm 2.28$ ), Shanghai ( $15.24 \pm 2.53$ ), Shandong ( $13.04 \pm 2.35$ ), Jiangsu ( $12.02 \pm 1.61$ ), Beijing ( $11.96 \pm 1.72$ ), Hebei ( $10.92 \pm 1.90$ ), Hong Kong ( $9.91 \pm 2.44$ ), and Henan ( $9.75 \pm 1.99$ ). Seasonally, the 12 provinces of China are extremely polluted in winter, six in autumn and spring, and one in summer.
- In terms of SO<sub>2</sub>, China's 10 provinces are categorized as extremely polluted provinces, including Shandong ( $20.62 \pm 6.33$ ), Tianjin ( $20.55 \pm 5.06$ ), Hebei ( $18.05 \pm 3.72$ ), Beijing ( $17.22 \pm 2.71$ ), Henan ( $17.15 \pm 4.15$ ), Shanxi ( $16.77 \pm 2.71$ ), Jiangsu ( $15.70 \pm 3.66$ ), Shanghai ( $15.69 \pm 4.81$ ), Anhui (Jiangsu ( $14.41 \pm 2.38$ ), and Liaoning ( $14.30 \pm 1.49$ ). Seasonally, the 17 provinces of China are extremely polluted in winter, nine in spring, and 10 in autumn.
- In China, high SO<sub>2</sub>/NO<sub>2</sub> ratio values (> 0.60) indicate that industry is the dominant source of SO<sub>2</sub> emissions which are relatively higher than NO<sub>2</sub> on a seasonal and annual basis.
- NO<sub>2</sub> (6%–66%) during the 12th FYP period (2011–2015) and SO<sub>2</sub> (3%–74%) during the 11th FYP period (2006–2010) were significantly decreased in China because of the implementation of strict air pollution control policies, like installing combined cycle technology, denitration facilities, desulfurization projects for coal-fired power plants and major industrial sectors.

nology, denitration facilities, desulfurization projects for coal-fired power plants and major industrial sectors.

The study is helpful in understanding the levels of NO<sub>2</sub> and SO<sub>2</sub> pollution and can be considered as a base document that supports the Chinese government's environmental policies.

**Supplementary Information** The online version contains supplementary material available at <https://doi.org/10.1007/s11869-024-01565-8>.

**Acknowledgements** The authors are thankful to NASA for making freely available the Aura-OMI-based total column NO<sub>2</sub> and SO<sub>2</sub> concentrations.

**Author's contribution statement** Md. Arfan Ali: Conceptualization, Data curation, Methodology, Formal analysis, Investigation, Validation, Visualization, Writing—original draft, Mazen E. Asiri, Md Nazrul Islam, Muhammad Bilal, Lama Alamri, Ayman Ghulam: Writing—review & editing.

**Funding** This work does not get any funding from any organization.

**Data availability** Data will be available on request.

## Declarations

**Ethics approval** Not applicable.

**Consent to participate** All authors consent to participate.

**Consent for publication** All authors consent to publish.

**Competing interests** The authors declare that they have no known competing financial interests or personal relationships that could have appeared to influence the work reported in this paper.

## References

- Abbass K, Qasim MZ, Song H et al (2022) A review of the global climate change impacts, adaptation, and sustainable mitigation measures. *Environ Sci Pollut Res* 29:42539–42559. <https://doi.org/10.1007/s11356-022-19718-6>
- Abdul Halim ND, Latif MT, Ahamad F, Dominick D, Chung JX, Juneng L, Khan MF (2018) The long-term assessment of air quality on an island in Malaysia. *Heliyon* 4:e01054. <https://doi.org/10.1016/j.heliyon.2018.e01054>
- Ali MA, Huang Z, Bilal M et al (2023a) Long-term PM<sub>2.5</sub> pollution over China: Identification of PM<sub>2.5</sub> pollution hotspots and source contributions. *Sci Total Environ* 893:164871. <https://doi.org/10.1016/j.scitotenv.2023.164871>
- Ali MA, Wang Y, Bilal M et al (2023b) Trace Gases over Land and Ocean Surfaces of China: Hotspots, Trends, and Source Contributions. *Earth Syst Environ* 7:801–819. <https://doi.org/10.1007/s41748-023-00354-0>
- Aneja VP, Agarwal A, Roelle PA et al (2001) Measurements and analysis of criteria pollutants in New Delhi, India. *Environ Int* 27:35–42. [https://doi.org/10.1016/S0160-4120\(01\)00051-4](https://doi.org/10.1016/S0160-4120(01)00051-4)
- Berglen TF (2004) A global model of the coupled sulfur/oxidant chemistry in the troposphere: the sulfur cycle. *J Geophys Res* 109:D19310. <https://doi.org/10.1029/2003JD003948>
- Bilal M, Mhawish A, Nichol JE et al (2021) Air pollution scenario over Pakistan: Characterization and ranking of extremely polluted cities

- using long-term concentrations of aerosols and trace gases. *Remote Sens Environ* 264:112617. <https://doi.org/10.1016/j.rse.2021.112617>
- Bovensmann H, Burrows JP, Buchwitz M, Frerick J, Noël S, Rozanov VV, Chance KV, Goede APH (1999) SCIAMACHY: mission objectives and measurement modes. *J Atmos Sci* 56:127–150. [https://doi.org/10.1175/1520-0469\(1999\)056%3c0127:SMOAMM%3e2.0.CO;2](https://doi.org/10.1175/1520-0469(1999)056%3c0127:SMOAMM%3e2.0.CO;2)
- Burrows JP, Weber M, Buchwitz M et al (1999) The Global Ozone Monitoring Experiment (GOME): mission concept and first scientific results. *J Atmos Sci* 56:151–175. [https://doi.org/10.1175/1520-0469\(1999\)056%3c0151:TGOMEG%3e2.0.CO;2](https://doi.org/10.1175/1520-0469(1999)056%3c0151:TGOMEG%3e2.0.CO;2)
- Callies J, Corpaccioli E, Eisinger M, Lefebvre A, Munro R, Perez-Albina A, Ricciarelli B, Calamai L, Gironi G, Veratti R, Otter G, Eschen M, van Riel L (2004) GOME-2 ozone instrument onboard the European METOP satellites. In: Vonder Haar TH, Huang HLA (eds) *Weather and environmental satellites*. <https://doi.org/10.1117/12.557860>
- Cai ZY, Yan X, Han SQ, Yao Q, Liu JL (2020) Transport Characteristics of Air Pollution in Tianjin Based on Weather Background. *Huan Jing Ke Xue* 41(11):4855–4863. <https://doi.org/10.13227/j.hjkk.202004252>
- Carey IM, Atkinson RW, Kent AJ et al (2013) Mortality associations with long-term exposure to outdoor air pollution in a national english cohort. *Am J Respir Crit Care Med* 187:1226–1233. <https://doi.org/10.1164/rccm.201210-1758OC>
- Carn SA, Fioletov VE, McLinden CA et al (2017) A decade of global volcanic SO<sub>2</sub> emissions measured from space. *Sci Rep* 7:44095. <https://doi.org/10.1038/srep44095>
- Celarier EA, Brinksma EJ, Gleason JF et al (2008) Validation of Ozone Monitoring Instrument nitrogen dioxide columns. *J Geophys Res* 2008:113. <https://doi.org/10.1029/2007JD008908>
- Chan CK, Yao X (2008) Air pollution in mega cities in China. *Atmos Environ* 42:1–42. <https://doi.org/10.1016/j.atmosenv.2007.09.003>
- Chang Y (2012) China Needs a Tighter PM<sub>2.5</sub> Limit and a Change in Priorities. *Environ Sci Technol* 46:7069–7070. <https://doi.org/10.1021/es3022705>
- Cheng MM, Jiang H, Guo Z (2012) Evaluation of long-term tropospheric NO<sub>2</sub> columns and the effect of different ecosystem in Yangtze River Delta. *Procedia Environ Sci* 13:1045–1056. <https://doi.org/10.1016/j.proenv.2012.01.098>
- Cheng Y, Wang S, Zhu J et al (2019) Surveillance of SO<sub>2</sub> and NO<sub>2</sub> from ship emissions by MAX-DOAS measurements and implication to compliance of fuel sulfur content. *Atmos Chem Phys* 19:13611–13626. <https://doi.org/10.5194/acp-2019-369>
- Dahiya S, Myllyvirta L (2019) Global SO<sub>2</sub> emission hotspot database RANKING THE WORLD'S WORST SOURCES OF SO<sub>2</sub> POLLUTION Content. Greenpeace Environment Trust. [https://www.greenpeace.org/static/planet4-africa-stateless/2019/08/5f139f4c-final-global-hotspot-and-emission-sources-for-so2\\_19th\\_august-2019.pdf](https://www.greenpeace.org/static/planet4-africa-stateless/2019/08/5f139f4c-final-global-hotspot-and-emission-sources-for-so2_19th_august-2019.pdf). Accessed 26 June 2023
- Damiani A, De Simone S, Rafanelli C, Cordero R, Laurenza M (2012) Three years of ground-based total ozone measurements in the Arctic: Comparison with OMI, GOME and SCIAMACHY satellite data. *Remote Sens Environ* 127:162–180
- de Leeuw G, van der AR, Bai J et al (2021) Air quality over China. *Remote Sens* 13:3542. <https://doi.org/10.3390/rs13173542>
- Dong GH, Zhang P, Sun B et al (2012) Long-term exposure to ambient air pollution and respiratory disease mortality in Shenyang, China: a 12-year population-based retrospective cohort study. *Respiration* 84:360–368. <https://doi.org/10.1159/000332930>
- Eisinger M, Burrows JP (1998) Tropospheric sulfur dioxide observed by the ERS-2 GOME instrument. *Geophys Res Lett* 25:4177–4180. <https://doi.org/10.1029/1998GL900128>
- Feng Z, Huang Y, Feng Y, Ogura N, Zhang F (2001) Chemical composition of precipitation in Beijing area, Northern China. *Water Air Soil Pollut* 125:345–356. <https://doi.org/10.1023/A:1005287102786>
- Forkel M, Carvalhais N, Verbesselt J et al (2013) Trend Change Detection in NDVI Time Series: Effects of Inter-Annual Variability and Methodology. *Remote Sens* 5:2113–2144. <https://doi.org/10.3390/rs5052113>
- Gao Y, Zhang M, Guo J, Xu L (2022) Impact of the oxidation of SO<sub>2</sub> by NO<sub>2</sub> on regional sulfate concentrations over the North China Plain. *Atmos Pollut Res* 13:1–12. <https://doi.org/10.1016/j.apr.2022.101337>
- Guo H, Gu X, Ma G et al (2019) Spatial and temporal variations of air quality and six air pollutants in China during 2015–2017. *Sci Rep* 9:1–11. <https://doi.org/10.1038/s41598-019-50655-6>
- Hao J, Zhu T, Fan X (2014) Indoor air pollution and its control in China. In: *Indoor air pollution. The handbook of environmental chemistry*, vol. 64. Springer, Berlin/Heidelberg, pp 145–170
- Haq ZU, Tariq S, Ali M (2015) Tropospheric NO<sub>2</sub> Trends over South Asia during the Last Decade (2004–2014) Using OMI Data. *Adv Meteorol* 2015:1–18. <https://doi.org/10.1155/2015/959284>
- He T, Tang Y, Cao R, Xia N, Li B, Du E (2023) Distinct urban-rural gradients of air NO<sub>2</sub> and SO<sub>2</sub> concentrations in response to emission reductions during 2015–2022 in Beijing, China. *Environ Pollut* 333:122021. <https://doi.org/10.1016/j.envpol.2023.122021>
- Hilboll A, Richter A, Burrows JP (2013) Long-term changes of tropospheric NO<sub>2</sub> over megacities derived from multiple satellite instruments. *Atmos Chem Phys Discuss* 13:4145–4169. <https://doi.org/10.5194/acp-13-4145-2013>
- Kendall MG (1975) *Rank correlation methods*, 4th edn. Charles Griffin, San Francisco, London
- Krotkov NA, McLinden CA, Li C et al (2016) Aura OMI observations of regional SO<sub>2</sub> and NO<sub>2</sub> pollution changes from 2005 to 2015. *Atmos Chem Phys Discuss* 16:4605–4629. <https://doi.org/10.5194/acp-16-4605-2016>
- Lamsal LN, Martin RV, Parrish DD, Krotkov NA (2013) Scaling Relationship for NO<sub>2</sub> Pollution and Urban Population Size: A Satellite Perspective. *Environ Sci Technol* 47:7855–7861. <https://doi.org/10.1021/es400744g>
- Lee DS, Köhler I, Grobler E et al (1997) Estimations of global no, emissions and their uncertainties. *Atmos Environ* 31:1735–1749. [https://doi.org/10.1016/S1352-2310\(96\)00327-5](https://doi.org/10.1016/S1352-2310(96)00327-5)
- Levelt P, Hilsenrath E, Leppelmeier G et al (2006a) Science objectives of the ozone monitoring instrument. *IEEE Trans Geosci Remote Sens* 44:1199–1208. <https://doi.org/10.1109/TGRS.2006.872336>
- Levelt P, Oord GVD, Dobber M et al (2006b) The ozone monitoring instrument. *IEEE Trans Geosci Remote Sens* 44:1093–1101. <https://doi.org/10.1109/TGRS.2006.872333>
- Levelt PF, Joiner J, Tamminen J et al (2018) The Ozone Monitoring Instrument: Overview of 14 years in space. *Atmos Chem Phys Discuss* 18:5699–5745. <https://doi.org/10.5194/acp-18-5699-2018>
- Li C, McLinden C, Fioletov V et al (2017a) India Is Overtaking China as the World's Largest Emitter of Anthropogenic Sulfur Dioxide. *Sci Rep* 7:14304. <https://doi.org/10.1038/s41598-017-14639-8>
- Li M, Zhang Q, Kurokawa J et al (2017b) MIX: a mosaic Asian anthropogenic emission inventory under the international collaboration framework of the MICS-Asia and HTAP. *Atmos Chem Phys* 17:935–963. <https://doi.org/10.5194/acp-17-935-2017>
- Lin JT, McElroy MB (2011) Detection from space of a reduction in anthropogenic emissions of nitrogen oxides during the Chinese economic downturn. *Atmos Chem Phys Discuss* 11:8171–8188. <https://doi.org/10.5194/acp-11-8171-2011>
- Lu Z, Streets D, de Foy B, Krotkov N (2013) Ozone Monitoring Instrument Observations of Interannual Increases in SO<sub>2</sub> Emissions from Indian Coal-Fired Power Plants during 2005–2012. *Environ Sci Technol* 47:13993–14000. <https://doi.org/10.1021/es4039648>
- Ma Z, Liu R, Liu Y, Bi J (2019) Effects of air pollution control policies on PM<sub>2.5</sub> pollution improvement in China from 2005 to 2017:

- a satellite-based perspective. *Atmos Chem Phys* 19:6861–6877. <https://doi.org/10.5194/acp-19-6861-2019>
- Mann HB (1945) Nonparametric tests against trend. *Econometrica* 13:245. <https://doi.org/10.2307/1907187>
- Meng ZY, Xu XB, Wang T et al (2010) Ambient sulfur dioxide, nitrogen dioxide, and ammonia at ten background and rural sites in China during 2007–2008. *Atmos Environ* 44:2625–2631. <https://doi.org/10.1016/j.atmosenv.2010.04.008>
- Mhawish A, Banerjee T, Sorek-Hamer M et al (2020) Estimation of High-Resolution PM<sub>2.5</sub> over the Indo-Gangetic Plain by Fusion of Satellite Data, Meteorology, and Land Use Variables. *Environ Sci Technol* 54:7891–7900. <https://doi.org/10.1021/acs.est.0c01769>
- Mhawish A, Sorek-Hamer M, Chatfield R et al (2021) Aerosol characteristics from earth observation systems: A comprehensive investigation over South Asia (2000–2019). *Remote Sens Environ* 259:112410. <https://doi.org/10.1016/j.rse.2021.112410>
- Munro R, Lang R, Klaes D et al (2016) The GOME-2 instrument on the Metop series of satellites: instrument design, calibration, and level 1 data processing—an overview. *Atmos Meas Tech* 9:1279–1301. <https://doi.org/10.5194/amt-9-1279-2016>
- Nirel R, Dayan U (2001) On the Ratio of Sulfur Dioxide to Nitrogen Oxides as an Indicator of Air Pollution Sources. *J Appl Meteorol* 40:1209–1222. [https://doi.org/10.1175/1520-0450\(2001\)040%3c1209:OTROSD%3e2.0.CO;2](https://doi.org/10.1175/1520-0450(2001)040%3c1209:OTROSD%3e2.0.CO;2)
- Qi H, Lin W, Xu X, Yu X, Ma Q (2012) Significant downward trend of SO<sub>2</sub> observed from 2005 to 2010 at a background station in the Yangtze Delta region, China. *Sci China Chem* 55:1451–1458. <https://doi.org/10.1007/s11426-012-4524-y>
- Richter A, Burrows JP (2002) Tropospheric NO<sub>2</sub> from GOME measurements. *Adv Sp Res* 29:1673–1683. [https://doi.org/10.1016/S0273-1177\(02\)00100-X](https://doi.org/10.1016/S0273-1177(02)00100-X)
- Saxena A (2023) Deteriorating Environmental Quality with Special Reference to War and Its Impact on Climate Change. *Natl Acad Sci Lett* 21:1–4. <https://doi.org/10.1007/s40009-023-01279-y>
- Seinfeld JH, Pandis SN (2006) Atmospheric chemistry and physics: from air pollution to climate change. In: Public administration review. Wiley, Hoboken
- Sen PK (1968) Estimates of the Regression Coefficient Based on Kendall's Tau. *J Am Stat Assoc* 63:1379–1389. <https://doi.org/10.1080/01621459.1968.10480934>
- Shon ZH, Kim K-H, Song SK (2011) Long-term trend in NO<sub>2</sub> and NO<sub>x</sub> levels and their emission ratio in relation to road traffic activities in East Asia. *Atmos Environ* 45:3120–3131
- Shukla S, Mbingwa G, Khanna S et al (2023) Environment and health hazards due to military metal pollution: A review. *Environ Nanotech Monitor Manag* 20:100857. <https://doi.org/10.1016/j.enmm.2023.100857>
- Slezakova K, Pires J, Martins F, Pereira M, Alvim-Ferraz M (2011) Identification of tobacco smoke components in indoor breathable particles by SEM–EDS. *Atmos Environ* 45:863–872. <https://doi.org/10.1016/j.atmosenv.2010.11.019>
- Sogacheva L, Rodriguez E, Kolmonen P et al (2018) Spatial and seasonal variations of aerosols over China from two decades of multi-satellite observations – Part 2: AOD time series for 1995–2017 combined from ATSR ADV and MODIS C6.1 and AOD tendency estimations. *Atmos Chem Phys* 18:16631–16652. <https://doi.org/10.5194/acp-18-16631-2018>
- Song R, Yang L, Liu M, Li C, Yang Y (2019) Spatiotemporal Distribution of Air Pollution Characteristics in Jiangsu Province, China. *Adv Meteorol* 1–14. <https://doi.org/10.1155/2019/5907673>
- Streets DG, Yarber KF, Woo JH, Carmichael GR (2003) Biomass burning in Asia: Annual and seasonal estimates and atmospheric emissions. *Glob Biogeochem Cycles* 17:4. <https://doi.org/10.1029/2003GB002040>
- Tan W, Liu C, Wang S et al (2018) Tropospheric NO<sub>2</sub>, SO<sub>2</sub>, and HCHO over the East China Sea, using ship-based MAX-DOAS observations and comparison with OMI and OMPS satellite data. *Atmos Chem Phys* 18:15387–15402. <https://doi.org/10.5194/acp-18-15387-2018>
- Tao Y, Huang W, Huang X et al (2012) Estimated acute effects of ambient Ozone and nitrogen dioxide on mortality in the Pearl River Delta of southern China. *Environ Health Perspect* 120:393–398. <https://doi.org/10.1289/ehp.1103715>
- Theil H (1992) A Rank-Invariant Method of Linear and Polynomial Regression Analysis BT - Henri Theil's Contributions to Economics and Econometrics: Econometric Theory and Methodology. Springer, Netherlands, pp 345–381
- Torres O, Tanskanen A, Veihelmann B et al (2007) Aerosols and surface UV products from Ozone Monitoring Instrument observations: An overview. *J Geophys Res* 112:D24S47. <https://doi.org/10.1029/2007JD008809>
- UNECE (2021) United Nations Economic Commission for Europe, Clean Air for Life. CH - 1211 Geneva 10, Switzerland. Available at [https://unece.org/sites/default/files/2021-06/Clean-air-for-life\\_eng\\_0.pdf](https://unece.org/sites/default/files/2021-06/Clean-air-for-life_eng_0.pdf). Accessed on 11 January 2023
- Veefkind JP, Aben I, McMullan K, Förster H, de Vries J, Otter G, Claas J, Eskes HJ, de Haan JF, Kleipool Q, van Weele M, Hasekamp O, Hoogeveen R, Landgraf J, Snel R, Tol P, Ingmann P, Voors R, Kruizinga B, Vink R, Visser H, Levelt PF (2012) TROPOMI on the ESA sentinel-5 precursor: a GMES mission for global observations of the atmospheric composition for climate, air quality and ozone layer applications. *Remote Sens Environ* 120:70–83. <https://doi.org/10.1016/j.rse.2011.09.027>
- Verbesselt J, Zeileis A, Herold M (2012) Near real-time disturbance detection using satellite image time series. *Remote Sens Environ* 123:98–108. <https://doi.org/10.1016/j.rse.2012.02.022>
- Wang YX (2004) Asian emissions of CO and NO<sub>x</sub>: Constraints from aircraft and Chinese station data. *J Geophys Res* 109:D24304. <https://doi.org/10.1029/2004JD005250>
- Wang S, Xing J, Chatani S et al (2011) Verification of anthropogenic emissions of China by satellite and ground observations. *Atmos Environ* 45:6347–6358. <https://doi.org/10.1016/j.atmosenv.2011.08.054>
- Wang SW, Zhang Q, Streets DG et al (2012) Growth in NO<sub>x</sub> emissions from power plants in China: Bottom-up estimates and satellite observations. *Atmos Chem Phys Discuss* 12:4429–4447. <https://doi.org/10.5194/acp-12-4429-2012>
- Wang Y, Ali MA, Bilal M et al (2021a) Identification of NO<sub>2</sub> and SO<sub>2</sub> Pollution Hotspots and Sources in Jiangsu Province of China. *Remote Sens* 13:3742. <https://doi.org/10.3390/rs13183742>
- Wang Y, Ali MA, Bilal M et al (2021b) Identification of Aerosol Pollution Hotspots in Jiangsu Province of China. *Remote Sens* 13:2842. <https://doi.org/10.3390/rs13142842>
- Wei J, Li Z, Wang J, Li C, Gupta P, Cribb M (2023) Ground-level gaseous pollutants (NO<sub>2</sub>, SO<sub>2</sub>, and CO) in China: daily seamless mapping and spatiotemporal variations. *Atmos Chem Phys* 23:1511–1532. <https://doi.org/10.5194/acp-23-1511-2023>
- Xiao X, Chang M, Guo P, Gu M, Li Y (2020) Analysis of air quality characteristics of Beijing–Tianjin–Hebei and its surrounding air pollution transport channel cities in China. *J Environ Sci* 87:213–227. <https://doi.org/10.1016/j.jes.2019.05.024>
- Xue R, Wang S, Li D et al (2020) Spatio-temporal variations in NO<sub>2</sub> and SO<sub>2</sub> over Shanghai and Chongming Eco-Island measured by Ozone Monitoring Instrument (OMI) during 2008–2017. *J Clean Prod* 258:120563. <https://doi.org/10.1016/j.jclepro.2020.120563>
- Yuan Y, Liu S, Castro R, Pan X (2012) PM<sub>2.5</sub> Monitoring and Mitigation in the Cities of China. *Environ Sci Technol* 46:3627–3628. <https://doi.org/10.1021/es300984j>
- Yue S, Hashino M (2003) Long term trends of annual and monthly precipitation in Japan. *JAWRA J Am Water Resour Assoc* 39:587–596. <https://doi.org/10.1111/j.1752-1688.2003.tb03677.x>

- Zhang L, Jacob DJ, Boersma KF et al (2008) Transpacific transport of ozone pollution and the effect of recent Asian emission increases on air quality in North America: An integrated analysis using satellite, aircraft, ozonesonde, and surface observations. *Atmos Chem Phys Discuss* 8:6117–6136. <https://doi.org/10.5194/acp-8-6117-2008>
- Zhang L, Lee CS, Zhang R, Chen L (2017) Spatial and temporal evaluation of long term trend (2005–2014) of OMI retrieved NO<sub>2</sub> and SO<sub>2</sub> concentrations in Henan Province, China. *Atmos Environ* 154:151–166. <https://doi.org/10.1016/j.atmosenv.2016.11.067>
- Zheng F, Yu T, Cheng T, Gu X, Guo H (2014) Intercomparison of tropospheric nitrogen dioxide retrieved from Ozone Monitoring Instrument over China. *Atmos Pollut Res* 5:686–695. <https://doi.org/10.5094/APR.2014.07>
- Zheng C, Zhao C, Li Y et al (2018) Spatial and temporal distribution of NO<sub>2</sub> and SO<sub>2</sub> in Inner Mongolia urban agglomeration obtained from satellite remote sensing and ground observations. *Atmos Environ* 188:50–59. <https://doi.org/10.1016/j.atmosenv.2018.06.029>

**Publisher's Note** Springer Nature remains neutral with regard to jurisdictional claims in published maps and institutional affiliations.

Springer Nature or its licensor (e.g. a society or other partner) holds exclusive rights to this article under a publishing agreement with the author(s) or other rightsholder(s); author self-archiving of the accepted manuscript version of this article is solely governed by the terms of such publishing agreement and applicable law.